Int. J. Plant Sci. 182(7):591–608. 2021.

1058-5893/2021/18207-0002$15.00 DOI: 10.1086/715508

PHYLOGENOMIC INSIGHTS INTO THE INDEPENDENT ORIGINS OF STERILE MARGINAL FLOWERS IN *VIBURNUM*

Brian Park[1,*] and Michael J. Donoghue†

*Department of Plant Biology, University of Georgia, Miller Plant Sciences Building, Athens, Georgia 30602, USA; and †Department of Ecology and Evolutionary Biology, Yale University, PO Box 208106, New Haven, Connecticut 06520, USA

Editor: Nicola G. Bergh

Premise of research. Many angiosperms produce floral displays with morphologically distinct flower types that together operate in pollinator attraction. In *Viburnum*, nine species in four widely separated subclades encircle their inflorescences with enlarged sterile marginal flowers (SMFs). Previous phylogenetic analyses of *Viburnum* were unable to resolve relationships within clades that contain species with SMFs, making it difficult to enumerate the origins/losses of SMFs and to identify possible environmental and organismal commonalities across these origins.

Methodology. We analyzed RAD-seq data to estimate phylogenetic relationships within each SMF subclade. We inferred demographic dynamics and historical gene flow to identify sources of phylogenetic discordance. Finally, we specifically tested hypotheses on how climate and plant architecture may have promoted the evolution of SMFs by inferring phylogenetic shifts and correlations across the origins of SMFs.

Pivotal results. Our analyses strongly support four origins of SMFs. In the cold-adapted *Opulus* and *Pseudotinus* lineages, rapid divergence and population size fluctuations coincided with the origins of SMFs. In the less cold-adapted *Euviburnum* clade, a rapid radiation in central China yielded one SMF-producing species. In the more subtropical *Lutescentia* lineage, the origin of SMFs appears to have coincided with a shift into cooler climates, and we found evidence of gene flow between partially sympatric species. SMFs never evolved in tropical or subtropical habitats, and shifts into colder climates may have promoted their origin. Three of the four origins of SMFs are associated with the evolution of distinctive plant growth patterns that amplify the floral display.

Conclusions. It appears that the evolution of SMFs was favored by a combination of shifts into colder climates and the evolution of branching patterns that increase the overall apparency of the floral display. However, our findings caution against the common assumption that the same causal factors underlie every instance of parallel evolution within a clade.

Keywords: parallel evolution, sterile marginal flowers, RAD-seq, phylogenomics, climatic niches, plant architecture.

Online enhancements: supplemental figures and table.

Introduction

A major aim of evolutionary research is to identify the causes underlying the repeated evolution of similar traits in distantly related lineages across the tree of life (Losos 2011; Stayton 2015). Once such independent evolutionary events have been identified phylogenetically, studies of repeated evolution typically involve analyses of correlated factors (e.g., Losos et al. 1998), tests of ecological function (Losos 2011), and attempts to identify the genetic and developmental factors underlying the trait of interest (Conte et al. 2012; Stern 2013). However, as we explain in the next paragraph, knowledge of correlated traits, current function, and proximate causes may be insufficient to fully characterize the environmental and organismal circumstances and the selective factors bearing on trait evolution.

Repeated evolution is typically assumed to be a consequence of the adaptation of distantly related species to similar environments (Losos 2011), with independent trait shifts promoted by movements into particular selective contexts or by the evolution of some underlying feature that might enable such shifts (Marazzi et al. 2012; Donoghue and Sanderson 2015). There are excellent examples of such studies among animals (e.g., the replicated reduction in bony armor in sticklebacks following shifts from marine to freshwater habitats; Bell et al. 1993; Cresko et al. 2004; Mobley et al. 2011) and among plants (e.g., the recurrent origins of C_4 photosynthesis in grasses triggered by movements into drier open areas; Sage 2001; Edwards and Smith 2010; Edwards et al. 2010; Spriggs et al. 2014). But seldom has it been possible to examine in detail every case of a repeatedly evolved

[1] Author for correspondence; email: brian.park@uga.edu.

Manuscript received March 2020; revised manuscript received March 2021; electronically published July 2, 2021.

trait within a clade that has been comprehensively sampled and to attempt to understand the population, environmental, and organismal circumstances surrounding each event. Although it is hoped that such studies will uncover a single causal factor that applies to every case, it is also possible that the "same" trait may have evolved in a variety of contexts and that evolution may have proceeded along somewhat different but ultimately overlapping trajectories.

Here we examine the multiple parallel origins of greatly enlarged and sterile flowers around the periphery of the inflorescences in *Viburnum* (sterile marginal flowers [SMFs]). Previous phylogenetic analyses support the hypothesis that flowers with such enlarged corollas have evolved independently in four distantly related *Viburnum* lineages (Donoghue et al. 2003; Clement et al. 2014; Spriggs et al. 2015). Recent experimental studies of the pollination ecology of two SMF-producing *Viburnum* species (*V. macrocephalum* and *V. lantanoides*) have shown that plants with intact SMFs experience significantly increased rates of insect visitation and fruit set compared with plants from which SMFs have been experimentally removed (Jin et al. 2010; Park et al. 2018). These studies provide evidence for the role of natural selection in driving the evolution of SMFs and suggest that pollination success may serve as the ultimate agent driving their independent origin.

It is well worth asking whether the origins of SMFs may be associated with pollinator shifts. *Viburnum* species both with and without SMFs appear to be generalists and are visited by a wide range of pollinating insects, including bees, flies, beetles, and, less frequently, other insects (Krannitz and Maun 1991*b*; Englund 1994; Kollman and Grubb 2002; Jin et al. 2010; Park et al. 2018; Wong Sato 2018). In any given species or setting, we imagine that only a few of these visitors are effective pollinators, but studies of *Viburnum* to date have not conclusively identified the major pollinating agent for any species. For example, the Holarctic SMF-bearing species *V. opulus* has been observed being visited by 49 species in populations planted in Canada (Krannitz and Maun 1991*b*) and by at least 70 species (35 families, 5 orders) in natural populations in Sweden, with the most important pollinators being solitary bees, hoverflies, and scarab beetles (Englund 1994). Similar patterns have also been observed in the Chinese SMF-bearing species *V. macrocephalum*, which is visited by insect species of 15 genera spanning five orders but is primarily serviced by bees and butterflies (Jin et al. 2010). In a study of nine native Japanese *Viburnum* species, SMF- and non-SMF-producing species were visited by a similar number of insect species (91 vs. 89 species, respectively), with the vast majority of visits by flies (50%), bees (29.2%), and beetles (16.7%; Wong Sato 2018). Furthermore, experimental removal of SMFs in the SMF-producing species did not alter the spectrum of insect visitors, suggesting that pollinator assemblages may vary by species but not depending on the presence or absence of SMFs (Wong Sato 2018). The existing pollinator data are insufficient to formally test whether shifts in pollinators have influenced the evolution of SMFs, but the available evidence does not suggest that the SMF-bearing species are specifically serviced by pollinators different from those that service species without SMFs.

If shifts in pollinators did not promote the evolution of SMFs, then what other factors may have contributed? One possibility that we explore here is that shifts into particular climatic circumstances played a role in facilitating the evolution of SMFs. Specifically, on the basis of our knowledge of the natural history of these species and our previous study of the SMF-bearing species *V. lantanoides* (Park et al. 2018), we hypothesize that occupation of colder climates favored the evolution of SMFs. The logic here is that SMFs could provide a particular advantage in attracting pollinating insects (and ultimately in fruit set and successful dispersal and/or establishment) where these insects may be limited, such as in cooler seasonal climates, especially when species flower early in the growing season. The advantage would be enhanced in areas where pollination success varies greatly from year to year (see Park et al. 2018 for an in-depth discussion of this hypothesis).

An additional factor contributing to the evolution of SMFs may be the arrangement and the density of inflorescences on the plant. In *Viburnum*, there are several evolutionarily derived branching architectures that have the effect of clustering the inflorescences on the plants. We hypothesize that these specialized branching patterns might have promoted the evolution of SMFs by displaying inflorescences in such a way as to increase apparency at the whole-plant level. The addition of SMFs might have a minor impact in species in which individual inflorescences are more scattered on the plant but could have a major impact when inflorescences are clustered to begin with. We test this branching architecture hypothesis here.

Until now, tests of the abovementioned hypotheses have been compromised by a lack of species-level resolution in the four SMF-containing clades that have been identified in prior phylogenetic studies of *Viburnum* (Donoghue et al. 2004; Winkworth and Donoghue 2004, 2005; Clement and Donoghue 2011; Clement et al. 2014; Spriggs et al. 2015). A recent study combining cpDNA and internal transcribed spacer (ITS) data from earlier studies with genome-wide RAD-seq data has provided greater resolution of relationships within these clades (Landis et al. 2021). However, to date, there have been no studies that have formally enumerated the number of origins (and possible losses) of SMFs across *Viburnum*, and there has also not been an exploration of the similarities and differences in the environments occupied by these species or of other possibly related morphological character changes associated with the origins of SMFs. Furthermore, there have been no attempts to identify the possible causes of phylogenetic discordance within the SMF-containing clades observed in earlier studies based on cpDNA and ITS data (see Winkworth and Donoghue 2005 and Clement et al. 2014 for a detailed discussion of such conflicts).

In this article, we first conduct comparative analyses using a recently inferred comprehensive *Viburnum* phylogeny (Landis et al. 2021) to test prior estimates of the number of gains (and potential losses) of SMFs and to characterize the climatological and growth form correlates of SMFs in a *Viburnum*-wide context. We then present targeted analyses of the RAD-seq data from Landis et al. (2021) to fully resolve relationships within each of the SMF clades and to identify the potential sources of phylogenetic discordance (i.e., incomplete lineage sorting [ILS] and introgression) that may have prevented such resolution in prior analyses. With this information in hand, we assess the hypotheses about the impact of climatic and organismal factors on the evolution of SMFs outlined above. Specifically, we ask whether SMF evolution coincides with transitions into colder climates and/or with the evolution of specialized branching patterns. Together, these analyses allow us to compare each instance of

the evolution of SMFs and to identify any common factors that may have promoted their evolution.

Material and Methods

Study System and Species

Viburnum is a clade of ~165 species of insect-pollinated shrubs and trees that produce flat-topped (or, more rarely, pyramid shaped) cymose inflorescences composed entirely of many (often hundreds) of small white (or cream colored; rarely, pink or yellow) perfect flowers with five stamens and radially symmetrical five-lobed corollas (Donoghue et al. 2003; Clement et al. 2014). *Viburnum* species appear to be largely self-incompatible (e.g., Krannitz and Maun 1991*a*; Park et al. 2018), and most fruit set is a result of outcrossing (Jin et al. 2010; Park et al. 2018). The inferior ovary matures into a single-seeded fleshy fruit (i.e., a drupe), and these are dispersed primarily by birds (Sinnott-Armstrong et al. 2020).

SMFs are produced by nine species distributed in four clades that have previously been shown to be distantly related within *Viburnum*, as follows: *Pseudotinus*, *Opulus*, *Euviburnum*, and *Lutescentia* (Clement et al. 2014; Spriggs et al. 2015). The presence, arrangement, and overall morphology of SMFs are remarkably constant across the nine species that produce them, despite the distant phylogenetic placement of the four clades containing these taxa. In these species, all individuals across all populations produce SMFs (i.e., we have never observed an inflorescence or individual plant without SMFs). Conversely, the occasional production of SMFs has never been recorded in species that do not produce them, and it is unlikely that a possible mutant could be misidentified, as the presence of SMFs is not the sole trait distinguishing these species. In general, two SMFs (sometimes more) are produced per lateral inflorescence ray (typically yielding a total of eight SMFs per inflorescence), and the addition of SMFs to an inflorescence effectively doubles the size (i.e., surface area) of the floral display (Park et al. 2018). SMFs are always characterized by enlarged corollas and highly reduced (typically entirely absent) stamens and have corolla lobes that are roughly five times larger in length than those of the fertile flowers in the center of the inflorescence (B. Park and M. J. Donoghue, personal observation). In all SMF-producing species, the SMFs generally develop and fully expand before (often by several days) the opening of the fertile flowers in the same inflorescence (see fig. 1*E* for an example in *V. macrocephalum*). Despite this overall constancy, there are some differences in the shapes and sizes of SMFs. For example, the seven SMF-producing species that are in the *Pseudotinus*, *Opulus*, and *Euviburnum*

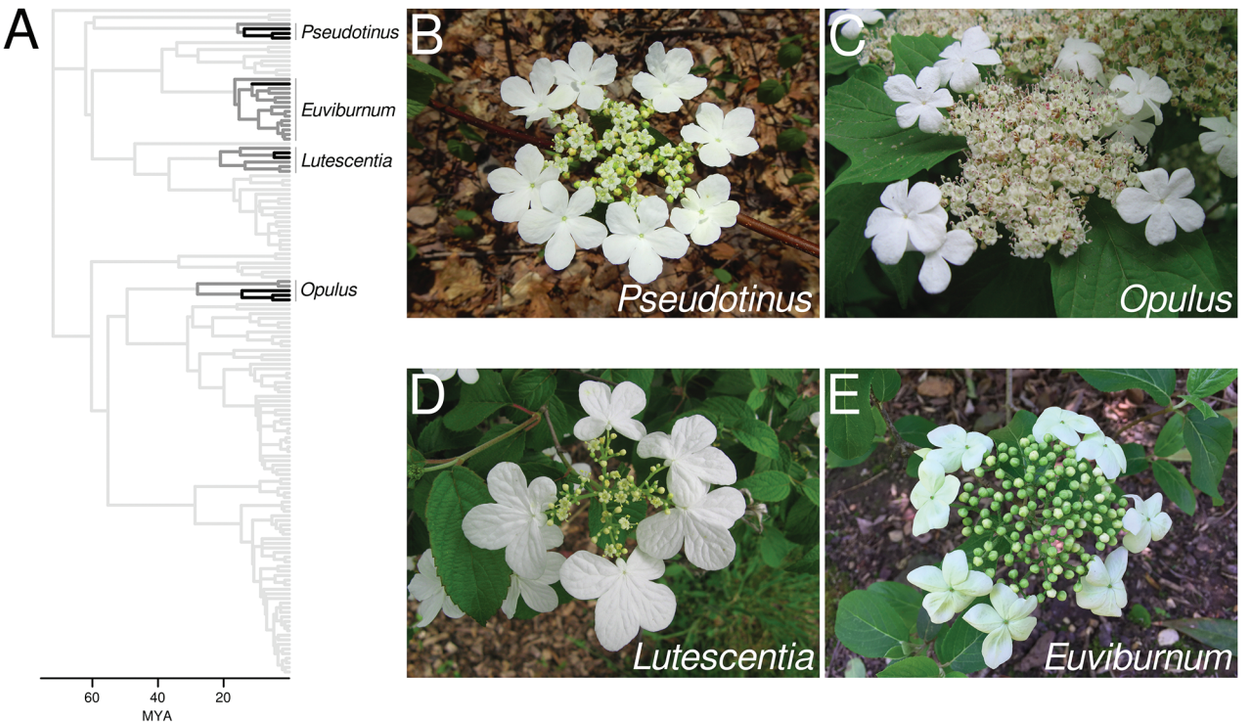

Fig. 1 Sterile marginal flowers (SMFs) evolved independently in four widely separated lineages within the *Viburnum* phylogeny (majority-rule consensus tree adapted from Landis et al. 2021). *A*, Clades within which SMFs evolved are indicated by the dark gray edges, with black edges indicating the SMF-producing species. Despite being distantly related to each other, the SMF-producing species produce remarkably similar floral displays, with only subtle differences in the shapes and sizes of SMFs between each clade. *B*, *Viburnum lantanoides* (pictured) and other members of the *Pseudotinus* clade produce SMFs with radially symmetrical corollas. *C*, *Viburnum sargentii* (pictured) and other members of the *Opulus* clade produce radially symmetrical SMFs that are slightly smaller in size than those in the other SMF clades (B. Park and M. J. Donoghue, personal observation). *D*, *Viburnum plicatum* (pictured) and *V. hanceanum* of *Lutescentia* produce SMFs with asymmetrical corollas. *E*, *Viburnum macrocephalum* (pictured) of *Euviburnum* also produces radially symmetrical corollas but with more dissected corolla lobes. Photographs by M. J. Donoghue.

clades produce SMFs with radially (or only slightly bilaterally) symmetrical corollas. By contrast, the two SMF species in *Lutescentia* produce SMFs with asymmetrical corollas where the ventral and lateral petals are much larger than the dorsal petals, which also differ from one another in size (fig. 1*D*). Mutant "snowball" forms of *V. opulus* (*Opulus*), *V. macrocephalum* (*Euviburnum*), and *V. plicatum* (*Lutescentia*) are propagated vegetatively and are widely used in horticulture (fig. S1; figs. S1–S3 are available online). These forms produce inflorescences composed entirely of sterile flowers, though these are typically somewhat smaller than they are in the "wild-type" form. Curiously, the snowball form of *V. plicatum* produces radially symmetrical sterile flowers, in contrast to the asymmetrical SMFs of its wild-type form.

Seven different patterns of branching have been described for *Viburnum* (Donoghue 1981, 1982; Edwards et al. 2014). Four of these are characterized by the production of only orthotropic (upward directed) shoots; these four types differ from one another primarily in the timing of branching relative to inflorescence production (Donoghue 1981, 1982). In these patterns, the inflorescences are spaced apart from one another and generally appear scattered on the plant (fig. 2*A*). Each of the other three branching patterns are derived within *Viburnum* (Edwards et al. 2014; fig. S2) and involve the production of specialized shoots that have the overall effect of clustering inflorescences in particular ways. Specifically, the "*opulus*" growth pattern (which characterizes the *Opulus* clade) is characterized by the production of different types of orthotropic shoots, with one form specialized for the production of terminal inflorescences. These reproductive shoots typically die back and are "replaced" by vegetative shoots that emerge from the axils of bud scales. This growth pattern tends to position a cluster of four or more inflorescences pointing upward at the same general level (fig. 2*B*). In the "*furcatum*" and "*plicatum*" branching patterns (which characterize the *Pseudotinus* and *Lutescentia* clades, respectively), there are orthotropic shoots and also specialized plagiotropic shoots that grow out from the main axis parallel to the ground. These two patterns differ from one another in the growth of the plagiotropic shoots. In the *plicatum* pattern, they are monopodial and grow out (for multiple seasons) from the terminal bud of the lateral branch. By contrast, in the *furcatum* pattern, the plagiotropic axes are sympodial; that is, the outward growth in the next season is from a lateral bud. These two patterns both eventually have the effect of positioning pairs of inflorescences side by side in a "double-file" pattern along the length of the plagiotropic axis (fig. 2*C*, 2*D*).

Viburnum-*Wide Analyses of Number of Origins, Environmental Settings, and Correlated Traits*

We conducted comparative analyses using a fossil-dated majority-rule consensus tree of *Viburnum* estimated from nine chloroplast, ITS, or RAD-seq loci (Landis et al. 2021). We pruned the phylogeny to 145 taxa (of 163 extant taxa) for which we were able to obtain sufficient georeferenced occurrence records for climatic analyses (see below). All analyses described in this section were conducted using this tree.

We estimated the number and phylogenetic placement of the origins of SMFs across *Viburnum*, and we conducted ancestral state reconstructions of SMFs under maximum likelihood (ML) using the rayDISC function in the R (R Core Team 2018) package corHMM (Beaulieu et al. 2013). We also conducted stochastic character mapping of SMFs (Nielsen 2002; Huelsenbeck et al. 2003) using the make.simmap function in the R package phytools (Revell 2011), generating 1000 character maps and estimating the number of transitions across these maps using the count.simmap function in phytools. Reconstructions were performed using Mk models with different transition rates: equal rates (ER), allowing for equal rates of gains and losses; all rates different (ARD), allowing rates of gains and losses to vary; and irreversible (IR), disallowing losses of SMFs. We complemented ML and stochastic character mapping with maximum parsimony

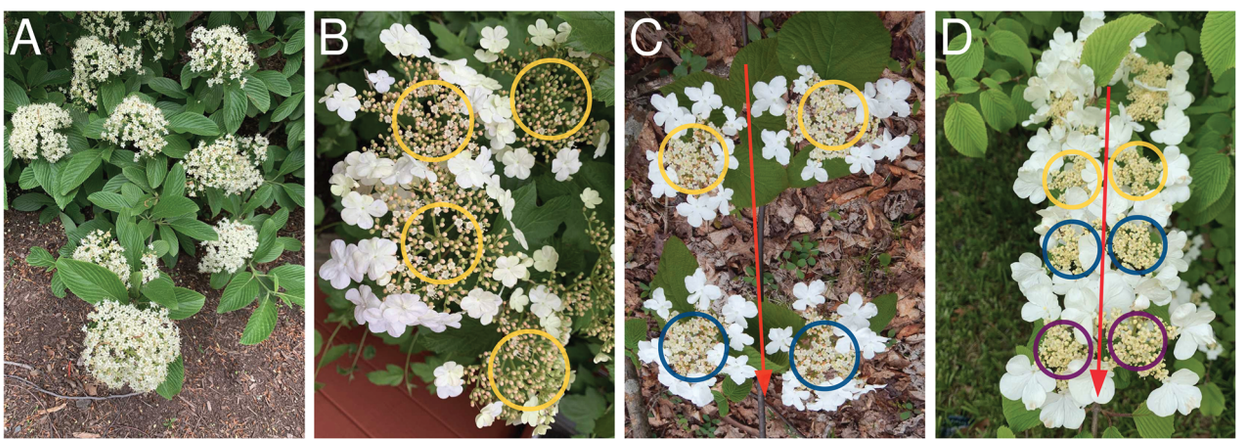

Fig. 2 In *Viburnum*, different growth patterns generate different arrangements of inflorescences on the plant. *A*, In *V. sieboldii*, all of the shoots are orthotropic, and the inflorescences are more or less evenly spread out on the plant. *B*, In *V. opulus* of the *Opulus* clade, the growth pattern involves two types of orthotropic shoots, and the inflorescences tend to be clustered in groups of four (marked by circles). *C*, *Viburnum lantanoides* of the *Pseudotinus* clade produces sympodial plagiotropic axes (arrow) along which inflorescences are borne in pairs (each pair marked by a particular color). *D*, *Viburnum plicatum* of the *Lutescentia* clade produces monopodial plagiotropic axes (arrow) along which inflorescences are borne in pairs (each pair marked by a particular color). In *C* and *D*, the inflorescences are borne in what is called a "double-file" arrangement. Photographs by M. J. Donoghue.

reconstructions in Mesquite version 3.4.0 (Maddison and Maddison 2018).

We investigated the climatological settings of SMF species across the broader *Viburnum* phylogeny. We first obtained georeferenced occurrence data for 145 species of *Viburnum* following the protocol of Edwards et al. (2017). Briefly, we collected species occurrence data from online databases (e.g., Global Biodiversity Information Facility [http://www.gbif.org/], Plant DNA Bank in Korea [http://pdbk.korea.ac.kr/], Flora of Nepal Database [http://umdb.um.u-tokyo.ac.jp/DShokubu/], etc.), previous studies (Edwards et al. 2017; Park and Donoghue 2019; Spriggs et al. 2019*a*, 2019*b*), and floras/taxonomic treatments (e.g., Hara 1983). Measurements of 19 BioClim variables (Fick and Hijmans 2017) at a 5-arc-minute resolution (~9 km × 9 km at the equator) were extracted for each occurrence using the R package raster (Hijmans 2017). Occurrences in the same grid cell and those outside the known distribution for each species were not included in downstream analyses. Using these data, we calculated the mean values for the 19 BioClim variables for each species and performed a phylogenetic principal components analysis (pPCA; Revell 2009) to determine the position of SMF species in the climatic niche space of *Viburnum*. We conducted a pPCA rather than a traditional PCA to account for nonindependence in trait values among species as a result of shared ancestry.

We used two methods to test for correlations between climate and SMFs. We first performed a phylogenetic ANOVA (phylANOVA; Garland et al. 1993) as implemented in phytools to determine whether SMF species differed significantly from non-SMF species. We performed these analyses using four BioClim variables that are easily interpretable and capture the general climatic features that determine climatic niches and distributions across *Viburnum*, as follows: mean annual temperature (Bio01), temperature annual range (Bio07), mean annual precipitation (Bio12), and precipitation seasonality (Bio15). For each test, we generated 1000 simulated data sets to determine significance. Considering that variables related to temperature seasonality (Bio04 [standard deviation of monthly temperature × 100] and Bio07) contributed heavily to the loadings on individual pPC axes (pPC1), we assessed the correlation between SMFs and seasonal climates using Pagel's (1994) test of correlated evolution between two binary characters following the approach of Edwards et al. (2017). Specifically, we focused on mean temperature of the coldest month (Bio06) and scored species as inhabiting seasonal (Bio06 < 0°C) or nonseasonal (Bio06 > 0°C) climates. On the basis of our field knowledge and published accounts, only one SMF species, *V. sympodiale*, was incorrectly scored as inhabiting nonseasonal climates based on our Bio06 character. This species occupies cool microclimates at high elevations in southern China and central Taiwan. Given the topographical complexity of these regions and the relatively coarse resolution of the climatic data (~9 km × 9 km at the equator), temperatures for occurrences of *V. sympodiale* are likely inflated, as they are an average between the cool climates at higher elevations and the subtropical/tropical climates at lower elevations in the same grid cell. Therefore, for the purposes of further analysis, we coded *V. sympodiale* as a seasonal species.

We also tested whether specialized growth forms are correlated with the production of SMFs. We used Pagel's (1994) test to determine whether these specialized growth forms (i.e., *opulus*, *plicatum*, and *furcatum*), with two different types of shoots, are correlated with the production of SMFs. To this end, we coded species for a binary character—the presence or absence of any of these specialized growth architectures—to test the hypothesis that inflorescence clustering at the whole-plant level may predispose plants to the evolution of SMFs.

Identifying Sources of Phylogenetic Discordance within the SMF Clades

The RAD-seq data processed and analyzed in this study were obtained from previous phylogenomic studies of *Viburnum* (Eaton et al. 2017; Landis et al. 2021). The samples used in the present study represent all nine SMF species in all four subclades in which SMFs are observed; all the available closest non-SMF-producing relatives of the SMF species and additional outgroups were also included in the separate analyses of the four relevant clades (table S1, available online).

We assembled raw demultiplexed reads from previous studies for each species into RAD loci and prepared for downstream analyses in ipyrad (Eaton 2014) version 0.7.22 (http://ipyrad.readthedocs.io/). Low-quality (more than four low-quality nucleotides at phred <33) and adapter-contaminated reads were filtered, and clusters with a minimum depth of six reads were assembled into RAD loci and clustered across samples at 90% nucleotide similarity. Two assemblies were generated at different sample coverage settings for phylogenomic analyses, as follows: a min4 assembly with loci shared across at least four samples and a min-ingroup assembly with loci shared across all ingroup samples. Because the recovery of RAD loci scales negatively with the number of samples (i.e., fewer loci are likely to be shared across a larger number of taxa; Eaton et al. 2017), we generated an assembly for the larger *Euviburnum* clade: a min-ingroup10 assembly in which loci shared across >75% of ingroup samples ($n = 10$ of 13 samples) were included for phylogenetic analyses. Additionally, for phylogenetic discordance analyses, owing to computational limitations, we generated a reduced_taxa assembly made up of loci from five species representing the major lineages within *Euviburnum* and two outgroup species.

We used supermatrix and species-tree approaches to estimate phylogenetic relationships within each subclade using data from all three assemblies. We first estimated ML phylogenies in RAxML version 8.2.5 (Stamatakis 2014) under the GTR+G substitution model and performed 100 nonparametric bootstrap replicates to assess support. We then estimated species trees in tetrad version 0.7.20. Tetrad is based on SVDquartets (Chifman and Kubatko 2014), which utilizes single-nucleotide polymorphism (SNP) data to estimate all possible quartets present in a given sample of taxa. These were subsequently joined into a supertree using the quartet-joining algorithm weighted quartet MaxCut (Avni et al. 2015). Support for the resulting species tree was assessed using 100 nonparametric bootstrap replicates.

We used three different approaches to measure the sources of phylogenetic discordance present in each SMF clade. First, we performed Bayesian concordance analysis (Ané et al. 2007; Baum 2007) to assess the extent of gene-tree discordance in each subclade. Gene trees were estimated in MrBayes version 3.2.2 (Huelsenbeck and Ronquist 2001) for loci shared among all taxa with at least two parsimony-informative sites. A posterior distribution of gene trees was produced for each locus by conducting

four replicate analyses, each running four Markov chain Monte Carlo (MCMC) chains for 5,000,000 generations, discarding the first 1,000,000 generations as burn-in, and sampling trees from every thousandth generation. Concordance factors (i.e., the proportion of loci supporting a given bipartition) and primary concordance trees (i.e., a topology representing the best-supported concordance factors) were estimated in BUCKy version 1.4.4 (Larget et al. 2010) at three values of expected gene-tree discordance ($\alpha = 0.1, 1, 10$). We conducted four replicate analyses for each α value, each with four MCMC chains run for 1,000,000 generations and with the first 20,000 generations discarded as burn-in. Results did not vary at different values of α, so we report the mean and 95% confidence estimates for the genome-wide concordance factors (CFs) at $\alpha = 1.0$.

Second, we detected signatures of introgression by performing ABBA-BABA tests (Green et al. 2010; Durand et al. 2011) and estimated the significance of each test by calculating *D* statistics (Eaton and Ree 2013). For each clade, we performed a series of tests based on the tree topology inferred through ML and species-tree analyses using the min4 data sets, assessing the significance of each test by performing 1000 bootstrap replicates following the SNP resampling procedure of Eaton and Ree (2013). Resulting *Z*-scores for each test were converted to two-tailed *P* values, and a Bonferroni correction was applied at $\alpha = 0.01$ to correct for multiple comparisons.

Third, we estimated divergence times and effective population sizes (N_e) for each node within each subclade using BPP version 3.3a (Rannala and Yang 2003) to explore the demographic factors (i.e., rapid diversification, population bottlenecks, etc.) that might underlie phylogenetic discordance. We used the a00 algorithm to estimate values of τ (coalescent branch length) and Θ (scaled mutation rate) using the tree topologies inferred through ML and species-tree analyses. For each subclade, we conducted four analyses using different combinations of priors for τ (2, 200 and 2, 2000) and Θ (2, 200 and 2, 2000) and then conducted eight independent runs for each analysis. For each run, we randomly selected 100 loci with at least two parsimony-informative SNPs and ran each MCMC chain for 100,000 generations, removing the first 10,000 generations as burn-in and sampling every subsequent 50 generations. The output of each run was examined in Tracer version 1.6 (Rambaut et al. 2014) to diagnose convergence and was then concatenated to obtain mean and 95% highest posterior density estimates for τ and Θ. Analyses were consistent across different τ and Θ priors, so we report results for $\tau = 2, 2000$ and $\Theta = 2, 2000$. Mean τ and Θ values were converted into absolute estimates of geological time and N_e assuming a conservative generation time (g) of 10 yr (Park and Donoghue 2019). Genome-wide substitution rates in *Viburnum* are unknown, so we assumed a mutation rate (μ) of 2.5×10^{-9} substitutions per site per year, which was the rate obtained for the woody plant *Populus* (Ingvarsson 2008).

Range Maps

Species distribution models for all of the SMF species and their closest relatives in each of the SMF subclades were generated using Maxent (Phillips et al. 2018) as implemented in the R package dismo (Hijmans et al. 2017). Models were estimated using default parameters with curated occurrences for each species (described above) and all 19 BioClim variables. Model performance was assessed using fivefold cross-validation. All models had an area under the curve > 0.8, indicating good model performance.

Results

Patterns across the Viburnum Phylogeny

Ancestral character reconstructions inferred a minimum of four gains of SMFs in the 145-taxon *Viburnum* phylogeny (fig. S3). ML reconstructions using different transition models were in agreement under the Akaike information criterion (AIC; $\Delta AIC < 2$): ER, log likelihood = −19.4, corrected AIC (AICc) = 40.9; ARD, log likelihood = −18.9, AICc = 42; and IR, log likelihood = −20, AICc = 42. ML reconstructions using IR identified an origin in the common ancestor of the SMF subclade within each clade: *V. lantanoides-sympodiale-furcatum* within *Pseudotinus*, *V. trilobum-opulus-sargentii* within *Opulus*, *V. hanceanum-plicatum* within *Lutescentia*, and *V. macrocephalum* within *Euviburnum*. ER and ARD reconstructions differed only with regard to the >0% probability of a placement of an origin of SMFs at the base of the entire *Pseudotinus* clade (fig. S3*A*, S3*B*), implying a loss of SMFs in *V. nervosum*.

Stochastic mapping yielded similar results, with the majority of the mappings inferring four gains of SMFs (ER = 78.8%, ARD = 54%, IR = 84.4%; data not shown). However, analyses varied by model in the inferred number of reversals. With ER, 42.8% of the maps identified no reversals within *Pseudotinus*, while 47.3% identified a reversal. With ARD, 8.8% of the maps identified no reversals, while 35.1% and 32% identified one or two reversals in the common ancestors of *Pseudotinus* and/or *Opulus*. Finally, parsimony reconstructions agreed with ML and stochastic mapping under IR in identifying exactly four gains of SMFs and zero losses.

pPCAs indicated that SMF species mostly occupy cooler, more seasonal climates (fig. 3*A*, 3*B*). SMF species scored positively on pPC1 (41.3% variance), where positive values are associated with greater temperature seasonality (Bio07) and colder winters and drier climates (Bio06 and Bio12, respectively). Along pPC1, *V. trilobum* (*Opulus*) was scored as being the most seasonal SMF species and was positioned with other species that occupy highly seasonal habitats (e.g., *V. burejaeticum* of northeast Asia; fig. 3*D*, 3*F*), while *V. hanceanum* (*Lutescentia*) was the least seasonal SMF species and was situated among species that occupy more subtropical or warm-temperate climates in Southeast Asia (e.g., the widespread *V. odoratissimum*; fig. 3*E*). However, SMF species were spread across pPC2 (21% variance), where positive values are associated with warmer summers (mean temperature of the warmest month [Bio05] and quarter [Bio10]) and drier winters (precipitation of the coldest quarter [Bio19]). Along pPC2, *V. hanceanum* (*Lutescentia*) was again situated with subtropical species (e.g., *V. odoratissimum*), while *V. trilobum* (*Opulus*) was positioned with far more cold-adapted species (e.g., *V. cassinoides* of eastern North America). Finally, SMF species as a whole scored negatively on pPC3 (13.8% variance), where positive values are associated with more insular tropical and island climates (isothermality [Bio03]) and with seasonally drier climates (precipitation of the driest month [Bio14]). All SMF species were positioned with other *Viburnum* species that occupy the temperate Northern Hemisphere, while Latin American and Southeast Asian species scored positively on pPC3 (fig. 3*B*).

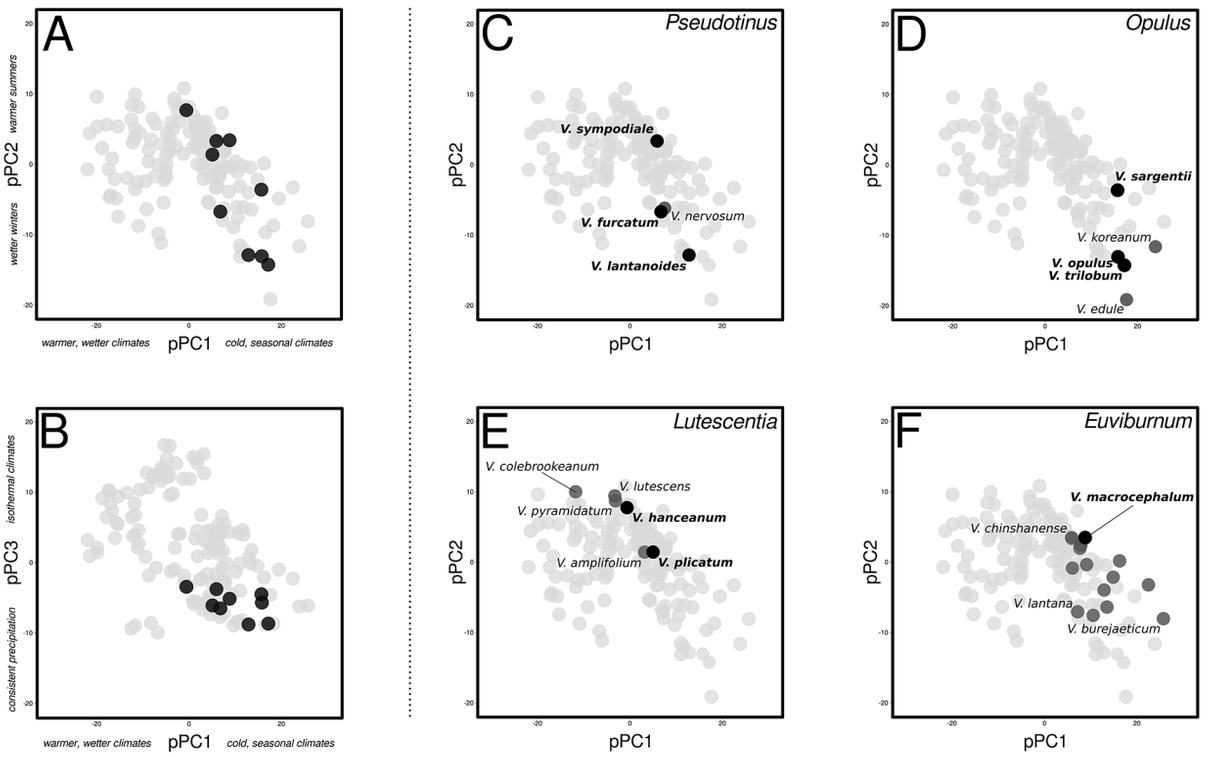

Fig. 3 Positions of sterile marginal flower (SMF)–producing species in multivariate climatic space generated by a phylogenetic principal components analysis (pPCA). Biplots of pPC1 against pPC2 (*A*) and pPC3 (*B*) show that the SMF-producing species (black circles) are clustered with other species (gray circles) that inhabit more seasonal climates. Positive values along pPC1 are associated with greater temperature seasonality (temperature annual range [Bio07]) and colder winters and drier climates (minimum temperature of the coldest month [Bio06] and mean annual precipitation [Bio12]). Along pPC2, positive values are associated with warmer summers (mean temperature of the warmest month [Bio05] and quarter [Bio10]) and drier winters (precipitation of the coldest quarter [Bio19]). Along pPC3, positive values are associated with more insular tropical and island climates (isothermality [Bio03]) and with seasonally drier climates (precipitation of the driest month [Bio14]). The positions of the SMF species (black circles) and their closest non-SMF relatives (dark gray circles) along pPC1 and pPC2 in each subclade are shown in *C*–*F*. *C*, *Pseudotinus*. *D*, *Opulus*. *E*, *Lutescentia*. *F*, *Euviburnum*.

When all SMF species were included in the analysis, the phylANOVA revealed no significant differences between SMF and non-SMF species in any of the BioClim variables (values given for selected variables): Bio01 (phylANOVA $F = 8.09$, $P = 0.127$), Bio07 (phylANOVA $F = 11.6$, $P = 0.07$), Bio12 (phylANOVA $F = 1.32$, $P = 0.55$), and Bio15 (phylANOVA $F = 2.33$, $P = 0.419$). Additionally, binary tests of correlated evolution between seasonal climates (scored using Bio06) and SMFs were not significant (Pagel's test: likelihood ratio = 4.97, $P = 0.083$). To explore this further, we carried out a set of sensitivity analyses asking whether particular species or clades might be responsible for these results. Specifically, we scored *V. hanceanum* and *V. plicatum* (the SMF-bearing taxa of *Lutescentia*) as though they were non-SMF species and found that there still were no significant differences between SMF and non-SMF species in Bio01, Bio07, Bio12, and Bio15. However, with this rescoring, we did find a significant difference between SMF and non-SMF species in Bio06 (analysis with the original scoring, phylANOVA $F = 11.6$, $P = 0.068$; analysis with the revised scoring, phylANOVA $F = 15.1$, $P = 0.043$). Additionally, with the revised scoring scheme, binary tests of correlated evolution between SMFs and seasonal climates were significant (Pagel's test: likelihood ratio = 9.81, $P = 0.007$). We carried out the same set of experiments with *V. macrocephalum* (the sole member of the *Euviburnum* clade with SMFs) rescored as not having SMFs (i.e., *V. macrocephalum* as well as *V. hanceanum* and *V. plicatum* scored as non-SMF species). Here, we found a significant association with SMFs and Bio06 (phylANOVA $F = 15.7$, $P = 0.049$) and seasonal climates (Pagel's test: likelihood ratio = 7.61, $P = 0.022$). Finally, tests of correlated evolution between specialized growth patterns and SMFs were also significant (likelihood ratio = 11.2, $P = 0.004$).

SMF Evolution within Pseudotinus

Pseudotinus contains three SMF-producing species (*V. sympodiale*, *V. furcatum*, and *V. lantanoides*) and one non-SMF species (*V. nervosum*). All of these species are cold adapted and inhabit cool mixed deciduous to boreal forests in the Himalayas and the Hengduan region of China (*V. nervosum*), the mountains of southern and central China and Taiwan (*V. sympodiale*), Korea and Japan (*V. furcatum*), and eastern North America (*V. lantanoides*). On average, 4.25×10^6 reads were sequenced per sample, with 23,857 and 7084 RAD loci recovered in the min4 and min-ingroup data sets, respectively (table S1).

ML and species-tree analyses conducted on the min4 and min-ingroup data sets yielded congruent well-supported topologies (fig. 4) and identified the Himalayan non-SMF species *V. nervosum* as the sister lineage to a well-supported clade of SMF species. Within the SMF clade, the cold-adapted eastern North American species *V. lantanoides* was resolved as sister to an eastern Asian clade composed of *V. sympodiale* and *V. furcatum*. ML analyses resolved all relationships within *Pseudotinus* with 100% bootstrap support (BS), while species-tree analyses resolved the relationship between *V. lantanoides* and *V. sympodiale-furcatum* with 97% and 91% BS using the min4 and min-ingroup data sets, respectively. The monophyly of the SMF species in all of the analyses provides strong evidence for a single origin of SMFs within *Pseudotinus* and is in agreement with the findings of Landis et al. (2021).

The primary concordance tree inferred using 1057 loci in BUCKy was congruent with the ML and species-tree phylogenies (fig. 4), and all clades within *Pseudotinus* were well supported (i.e., there were no conflicting splits with overlapping 95% confidence intervals [CIs]). The monophyly of *Pseudotinus* and the sister species relationship between *V. sympodiale* and *V. furcatum* were supported with CF > 0.9 (CF = 0.999, 95% CI = 0.997–1.00 and CF = 0.964, 95% CI = 0.924–0.991, respectively). However, the split between *V. nervosum* and *V. lantanoides-sympodiale-furcatum* was not as well supported (CF = 0.647, 95% CI = 0.567–0.725). This is likely a function of the short internode subtending the SMF clade resolved in the ML analyses (data not shown) and the <100% BS obtained in the species-tree analyses. A number of alternative placements of *V. nervosum* and *V. lantanoides* were supported with CF > 0.10, as follows: a sister species relationship between *V. nervosum* and *V. lantanoides* (CF = 0.182, 95% CI = 0.123–0.247) and *V. lantanoides* as sister to *V. nervosum-sympodiale-furcatum* (CF = 0.148, 95% CI = 0.085–0.216).

ABBA-BABA tests performed using 1969 loci did not identify any significant instances of gene flow within *Pseudotinus* ($Z < 1.0$ and $P > 0.05$ for all tests; 10 tests total), indicating that phylogenetic discordance is not the result of introgression. Instead, the divergence times and effective population sizes estimated with BPP suggest that this may be due to incomplete lineage sorting (table 1). This is apparent in the overlapping estimates for the crown age of *Pseudotinus* (10.1 mya, 95% CI = 6.36–13.9 mya) and the divergence between *V. nervosum* and the SMF species (9.10 mya, 95% CI = 5.80–12.6 mya). Furthermore, there was an estimated 3.5-fold reduction in effective population size from the ancestor of *Pseudotinus* (N_e = 69.7 × 10^3, 95% CI = 41.5 × 10^3–98.5 × 10^3) to the ancestor of the SMF species (N_e = 20.7 × 10^3, 95% CI = 16.1 × 10^3–46.3 × 10^3). Thus, a history of rapid speciation and fluctuations in population sizes (patterns consistent with ILS) likely underlies phylogenetic discordance in *Pseudotinus*.

SMF Evolution within Opulus

The *Opulus* clade contains three widely distributed SMF-producing species that differ only subtly in morphology but have widely disjunct distributions (*V. trilobum* in North America, *V. opulus* in Europe, and *V. sargentii* in northeast Asia) and a pair of non-SMF species that are disjunct across the Bering Strait (*V. koreanum* and *V. edule*). These species inhabit some of the coldest forests occupied by any *Viburnum* species, as reflected in their circumboreal distribution in mixed deciduous and boreal forests at high latitudes. The rarely collected *V. koreanum* was not included in our analyses, as RAD-seq data were not available for this species. Other analyses have shown that it recently diverged from its sister species *V. edule* (Clement and Donoghue 2011; Spriggs et al. 2015; Landis et al. 2021).

On average, 2.94 × 10^6 reads and 104,764 loci were recovered per sample. Clustering across samples yielded 87,087 loci, with 31,277 loci (33,087 parsimony-informative sites) in the min4 data set and 8551 loci (8232 parsimony-informative sites) in the min-ingroup data set. The total amount of missing data in the min4 and min-ingroup data sets was 23.8% and 13.6%, respectively (table S1).

Phylogenetic patterns in *Opulus* mirrored those observed in *Pseudotinus*. ML and species-tree analyses conducted on both data sets yielded congruent well-supported topologies (fig. 5) and identified the non-SMF North American boreal species *V.*

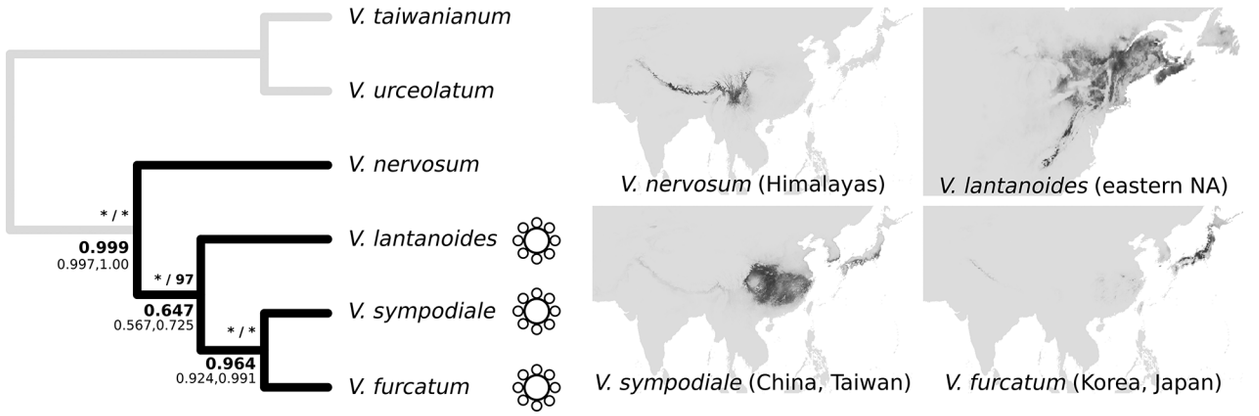

Fig. 4 *Pseudotinus* phylogeny inferred from RAD-seq data. Species of *Pseudotinus* are indicated by black edges, and outgroup species are indicated by light gray edges; illustrated inflorescences denote sterile marginal flower–producing species. Bootstrap support (BS) values for maximum likelihood and species-tree analyses of the min4 data set are denoted above each node; asterisks denote 100% BS. Mean concordance factors (in bold) and 95% confidence intervals are displayed below each node. Range maps for species of *Pseudotinus* estimated using Maxent are shown on the right. NA = North America.

Table 1

Divergence Times (t) and Effective Population Sizes (N_e) Estimated in BPP for *Viburnum*

Clade, parameter, species	Mean	Lower 95% CI	Upper 95% CI
Pseudotinus:			
t ($\times 10^6$ yr):			
taiw, urce, nerv, lant, symp, furc	45.6	28.8	65.2
nerv, lant, symp, furc	10.1	6.36	13.9
lant, symp, furc	9.10	5.80	12.6
symp, furc	4.84	1.42	8.24
N_e ($\times 10^3$):			
taiw, urce, nerv, lant, symp, furc	82.8	10.3	140
nerv, lant, symp, furc	69.7	41.5	98.5
lant, symp, furc	20.7	16.1	46.3
symp, furc	29.7	5.19	56.4
Opulus:			
t ($\times 10^6$ yr):			
cyli, acer, edul, tril, opul, sarg	40.4	25.2	59.2
edul, tril, opul, sarg	9.56	5.72	13.8
tril, opul, sarg	8.76	5.16	12.7
opul, sarg	7.28	3.93	10.8
N_e ($\times 10^3$):			
cyli, acer, edul, tril, opul, sarg	88.8	17.8	161
edul, tril, opul, sarg	72.2	40.2	106
tril, opul, sarg	19.1	1.66	41
opul, sarg	21.0	12.3	44
Lutescentia:			
t ($\times 10^6$ yr):			
farr, sieb, lute, ampl, hanc, plic	30.8	23.2	38.7
lute, ampl, hanc, plic	22.8	18.3	27.5
lute, ampl	18.6	9.56	25.3
hanc, plic	17.4	14.1	24.9
N_e ($\times 10^3$):			
farr, sieb, lute, ampl, hanc, plic	126	79.3	172
lute, ampl, hanc, plic	32.7	6.34	62.2
lute, ampl	30.9	1.77	79.3
hanc, plic	37.1	2.50	89.7
Euviburnum:			
t ($\times 10^6$ yr):			
punc, cass, coti, macr, carl, lant, rhyt	44.4	32.6	57.6
coti, macr, carl, lant, rhyt	20.4	16.0	25.6
macr, carl, lant, rhyt	20.1	15.8	25.3
macr, carl	19.0	14.1	24.9
lant, rhyt	16.4	6.20	23.8
N_e ($\times 10^3$):			
punc, cass, coti, macr, carl, lant, rhyt	87.1	45.4	128
coti, macr, carl, lant, rhyt	47.2	28.0	67.3
macr, carl, lant, rhyt	16.0	1.58	34.2
macr, carl	16.8	1.43	36.6
lant, rhyt	27.8	1.77	72.7

Note. *Pseudotinus*: taiw = *V. taiwanianum*; urce = *V. urceolatum*; nerv = *V. nervosum*; lant = *V. lantanoides*; symp = *V. sympodiale*; furc = *V. furcatum*. *Opulus*: cyli = *V. cylindricum*; acer = *V. acerifolium*; edul = *V. edule*; tril = *V. trilobum*; opul = *V. opulus*; sarg = *V. sargentii*. *Lutescentia*: farr = *V. farreri*; sieb = *V. sieboldii*; lute = *V. lutescens*; ampl = *V. amplifolium*; hanc = *V. hanceanum*; plic = *V. plicatum*. *Euviburnum*: punc = *V. punctatum*; cass = *V. cassinoides*; coti = *V. cotinifolium*; macr = *V. macrocephalum*; carl = *V. carlesii*; lant = *V. lantana*; rhyt = *V. rhytidophyllum*. CI = confidence interval.

edule as the sister lineage to a clade of SMF species composed of *V. trilobum*, *V. opulus*, and *V. sargentii*. As with the three SMF-bearing species in *Pseudotinus*, the eastern North American species *V. trilobum* was resolved as sister to a clade composed of two cold-adapted Old World species: *V. opulus* (northern and central Europe) and *V. sargentii* (northeast Asia). In contrast to *Pseudotinus*, all analyses resolved relationships within *Opulus* with 100% BS. Unequivocal support for the monophyly of the SMF species in *Opulus* provides strong evidence for a single origin of SMFs in the ancestor of *V. trilobum-opulus-sargentii* and agrees with the findings of Landis et al. (2021).

The primary concordance tree inferred using 1502 loci in BUCKy was in agreement with the topologies estimated under ML and in the species-tree analyses (fig. 5). As in *Pseudotinus*, all splits within *Opulus* were well supported. The monophyly of *Opulus* and the resolution of an SMF clade within *Opulus*

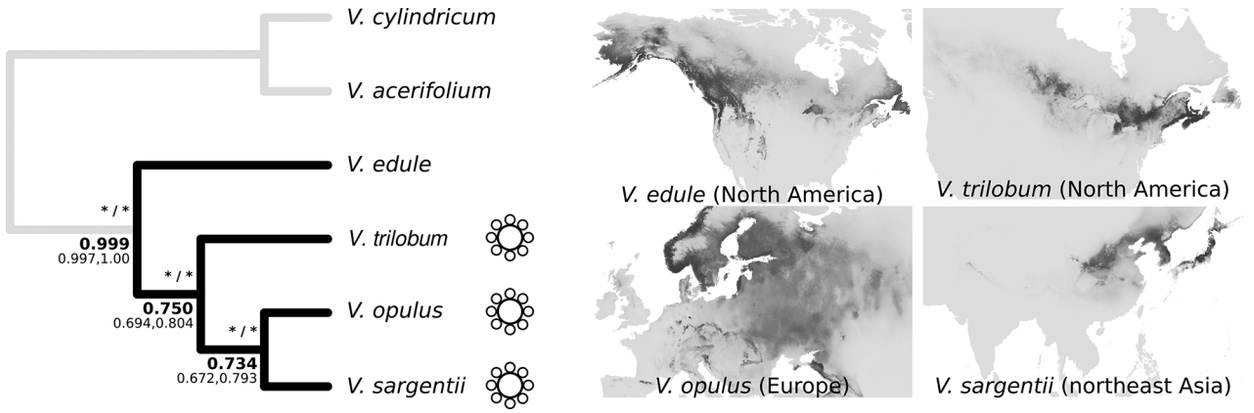

Fig. 5 *Opulus* phylogeny inferred from RAD-seq data. Species of *Opulus* are indicated by black edges, and outgroup species are indicated by light gray edges; illustrated inflorescences denote sterile marginal flower–producing species. Bootstrap support (BS) values for maximum likelihood and species-tree analyses of the min4 data set are displayed above each node; asterisks denote 100% BS. Mean concordance factors (in bold) and 95% confidence intervals are displayed below each node. Range maps for species of *Opulus* estimated using Maxent are shown on the right.

were resolved with high confidence (CF = 0.999, 95% CI = 0.997–1.00). The divergence between *V. trilobum* and *V. opulus-sargentii* and the sister species relationship between *V. opulus* and *V. sargentii* were supported with CF > 0.7 (CF = 0.750, 95% CI = 0.694–0.804 and CF = 0.734, 95% CI = 0.672–0.793, respectively). However, a number of alternative placements of *V. trilobum* were supported with CF > 0.10, as follows: a sister species relationship between *V. trilobum* and *V. sargentii* (CF = 0.161, 95% CI = 0.110–0.215), *V. trilobum* as sister to *V. edule-opulus-sargentii* (CF = 0.122, 95% CI = 0.080–0.122), and *V. trilobum* as sister to *V. edule* (CF = 0.114, 95% CI = 0.073–0.159).

ABBA-BABA tests performed on 3896 loci did not identify a signature of gene flow within *Opulus* ($Z = 0.174$, 1.61, $P > 0.05$ for all tests; 10 tests total), indicating that introgression is not a likely source of phylogenetic discordance in *Opulus*. As with *Pseudotinus*, demographic reconstructions in BPP, showing rapid divergences and population size fluctuations, suggested that ILS is more likely (table 1). The crown age of *Opulus* (9.56 mya, 95% CI = 5.72–13.8 mya) overlapped with the divergence time between *V. edule* and the SMF species (8.76 mya, 95% CI = 5.16–12.7 mya), consistent with the short internode subtending *V. trilobum-opulus-sargentii* inferred in ML analyses (data not shown). Furthermore, there was an estimated 3.5-fold reduction in effective population size from the most recent common ancestor of *Opulus* ($N_e = 72.2 \times 10^3$, 95% CI = 40.2×10^3–106×10^3) to the ancestor of the SMF clade ($N_e = 19.1 \times 10^3$, 95% CI = 0.166×10^3–40.1×10^3).

SMF Evolution within Lutescentia

Lutescentia contains approximately six species, two producing SMFs (*V. hanceanum* and *V. plicatum*) and four lacking SMFs (*V. lutescens*, *V. colebrookeanum*, *V. pyramidatum*, and *V. amplifolium*). The non-SMF species occupy warm subtropical forests in Southeast Asia and west to India (e.g., *V. colebrookeanum*; Bio06 = 10.8°C), while the SMF species inhabit relatively cooler forests in southern China and Taiwan (*V. hanceanum*; Bio06 = 5.8°C) and from central China to Japan (*V. plicatum*; Bio06 = −1.26°C). We did not have sufficient RAD-seq data for *V. colebrookeanum* (<200,000 reads) and did not have any RAD-seq data for the rarely collected taxa *V. garrettii* and *V. junghunii*, so we did not include these species in our analyses. Furthermore, we did not include *V. pyramidatum* in our analyses, as we consider it to be included in and probably synonymous with the *V. lutescens* lineage.

On average, 2.63×10^6 reads were sequenced and 101,101 loci were recovered per sample, with 85,375 loci recovered across samples. The min4 data set was composed of 31,854 loci (25,230 parsimony-informative sites), and the min-ingroup data set included 13,021 loci (10,304 parsimony-informative sites). The total amount of missing data in the min4 and min-ingroup data sets was 24.9% and 18.4%, respectively (table S1).

ML and species-tree analyses across data sets were congruent (fig. 6) and unequivocally resolved two clades within *Lutescentia*. One is composed of the widely distributed *V. lutescens* and *V. amplifolium* from Yunnan, and the other contains the two SMF species *V. hanceanum* and *V. plicatum*. The monophyly of the SMF species indicates that SMFs evolved once in *Lutescentia*, agreeing with the findings of Landis et al. (2021). We note that the four non-SMF species of *Lutescentia* in Landis et al. (2021) that are not included here (for the reasons described above) were found by Landis et al. (2021) to fall outside the *V. hanceanum*–*V. plicatum* clade.

As in *Pseudotinus* and *Opulus*, relationships within *Lutescentia* were well supported, and the primary concordance tree inferred using 1057 loci was congruent with the ML and species-tree topologies (fig. 6). There was strong support for the monophyly of *Lutescentia* itself (CF = 0.995, 95% CI = 0.98–0.99) and for the grouping of *V. lutescens-amplifolium* and of *V. hanceanum-plicatum* (CF = 0.796, 95% CI = 0.732–0.868 and CF = 0.774, 95% CI = 0.710–0.836, respectively). Two alternative placements of *V. lutescens* and *V. plicatum* as the earliest-diverging lineage within *Lutescentia* were supported with a CF of ~0.10: *V. plicatum* with CF = 0.114 and 95% CI = 0.073–0.159 and *V. lutescens* with CF = 0.091 and 95% CI = 0.045–0.144.

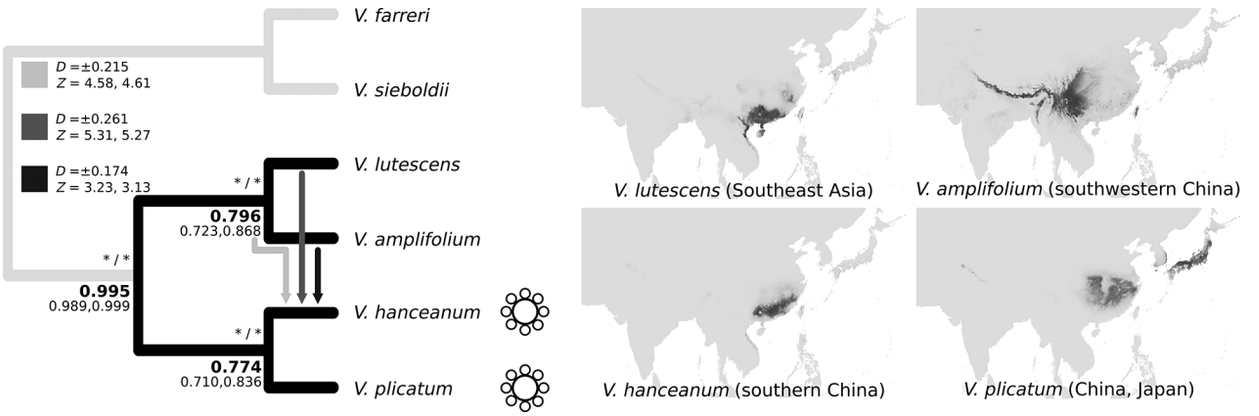

Fig. 6 *Lutescentia* phylogeny inferred from RAD-seq data. Species of *Lutescentia* are indicated by black edges, and outgroup species are indicated by light gray edges; illustrated inflorescences denote sterile marginal flower–producing species. Bootstrap support (BS) values for maximum likelihood and species-tree analyses of the min4 data set are displayed above each node; asterisks denote 100% BS. Mean concordance factors (in bold) and 95% confidence intervals are displayed below each node. Arrows denote gene flow from *Viburnum lutescens* (dark gray arrow), *V. amplifolium* (black arrow), and the common ancestor of *V. lutescens-amplifolium* (light gray arrow) into *V. hanceanum*. For each instance of gene flow, *D* statistics and *Z*-scores are reported next to the boxes corresponding to each colored arrow. Range maps for species of *Lutescentia* estimated using Maxent are shown on the right.

Multiple ABBA-BABA tests conducted on 3225 loci identified significant signatures of gene flow from *V. lutescens*, *V. amplifolium*, and the ancestor of *V. lutescens-amplifolium* into *V. hanceanum* (fig. 6). When *V. hanceanum* was treated as either the P1 or P2 (recipient) lineage, the most significant gene flow was from *V. lutescens* ($D = \pm 0.261$, $Z = 5.31$, 5.27; $P < 0.001$), followed by the ancestor of *V. lutescens* and *V. amplifolium* ($D = \pm 0.215$, $Z = 4.58$, 4.61; $P < 0.001$) and then *V. amplifolium* ($D = \pm 0.174$, $Z = 3.23$, 3.13; $P = 0.002$). Tests performed in the opposite direction (i.e., with *V. hanceanum* treated as the donor, P3, lineage) were not significant. Gene flow into *V. hanceanum* from these lineages makes sense considering that *V. lutescens*, *V. amplifolium*, and *V. hanceanum* have overlapping geographic distributions (fig. 6) and that *V. hanceanum* is an octoploid (2n = 72; Egolf 1956, 1962; Moeglein et al. 2020), which suggests that there may have been hybridization in its past.

Divergence times and population sizes estimated from 1057 loci in BPP (table 1) indicate that the crown age of *Lutescentia* (22.8 mya, 95% CI = 18.3–27.5 mya) overlaps somewhat with the establishment of the non-SMF clade (*V. lutescens* and *V. amplifolium*: 18.6 mya, 95% CI = 9.56–25.3 mya) and the SMF clade (*V. hanceanum* and *V. plicatum*: 17.4 mya, 95% CI = 14.1–24.9 mya). In contrast to *Pseudotinus*, *Opulus*, and *Euviburnum* (see below), there was no notable reduction in effective population size in either the common ancestor of *V. lutescens-amplifolium* or the ancestor of *V. hanceanum-plicatum* following their divergence (table 1). Taken together, these findings suggest that introgression, rather than ILS, underlies phylogenetic discordance in *Lutescentia*.

SMF Evolution within Euviburnum

Euviburnum contains ~15 species, only one of which produces SMFs (*V. macrocephalum* of central and eastern China). This is a small radiation in which the species diversity is highest in cool deciduous forests in central China. Two species are found in northeast Asia/Siberia (*V. burejaeticum* and *V. mongolicum*), one is found in the western Himalayas (*V. cotinifolium*), and one is broadly distributed in western and central Europe (*V. lantana*). We could not include *V. burejaeticum*, *V. mongolicum*, and *V. maculatum* in our analyses because of a lack of RAD-seq data, but other analyses indicate that these species form a clade with *V. lantana* (Spriggs et al. 2015; Landis et al. 2021).

On average, 2.43×10^6 reads and 81,282 loci were recovered per sample. Clustering across samples yielded 132,409 loci, with 78,871 loci (124,902 parsimony-informative sites) in the min4 data set and 13,971 loci (8232 parsimony-informative sites) in the min-ingroup10 data set. The total amount of missing data in the min4 and min-ingroup10 data sets was 47.2% and 22.3%, respectively (table S1).

ML and species-tree analyses conducted on the min4 and min-ingroup10 data sets identified three major divergences within *Euviburnum* (fig. 7*A*). The Himalayan species, *V. cotinifolium*, was resolved as the sister lineage to a clade containing the rest of *Euviburnum*, with varying degrees of BS: min 4 = 100% (ML) and min4 = 98% (species tree) and min-ingroup10 = 95% (ML) and min-ingroup10 = 86% (species tree). Relationships within *Euviburnum* are complicated, but two major clades were resolved with unequivocal support. One clade is composed of the Chinese SMF species *V. macrocephalum* and its sister group, containing species distributed from montane China into Korea and Japan (Yang et al. 2011), as follows: *V. schensianum* (northern Sichuan to Shandong), *V. utile* (Sichuan to Henan), *V. congestum* (Yunnan to Gansu), and *V. bitchiuense* and *V. carlesii* (Korea and Japan). Relationships in this clade are well resolved; however, the placement of *V. macrocephalum* is not well supported in species-tree analyses (53% and 51% BS). The second clade is composed of the European species *V. lantana*, which is sister to a clade containing several species in southwestern and central China (Yang et al. 2011), as follows: *V. chinshanense* (Yunnan to Shaanxi) and *V. buddleifolium* (Hubei), *V. rhytidophyllum* (Guizhou to Shaanxi),

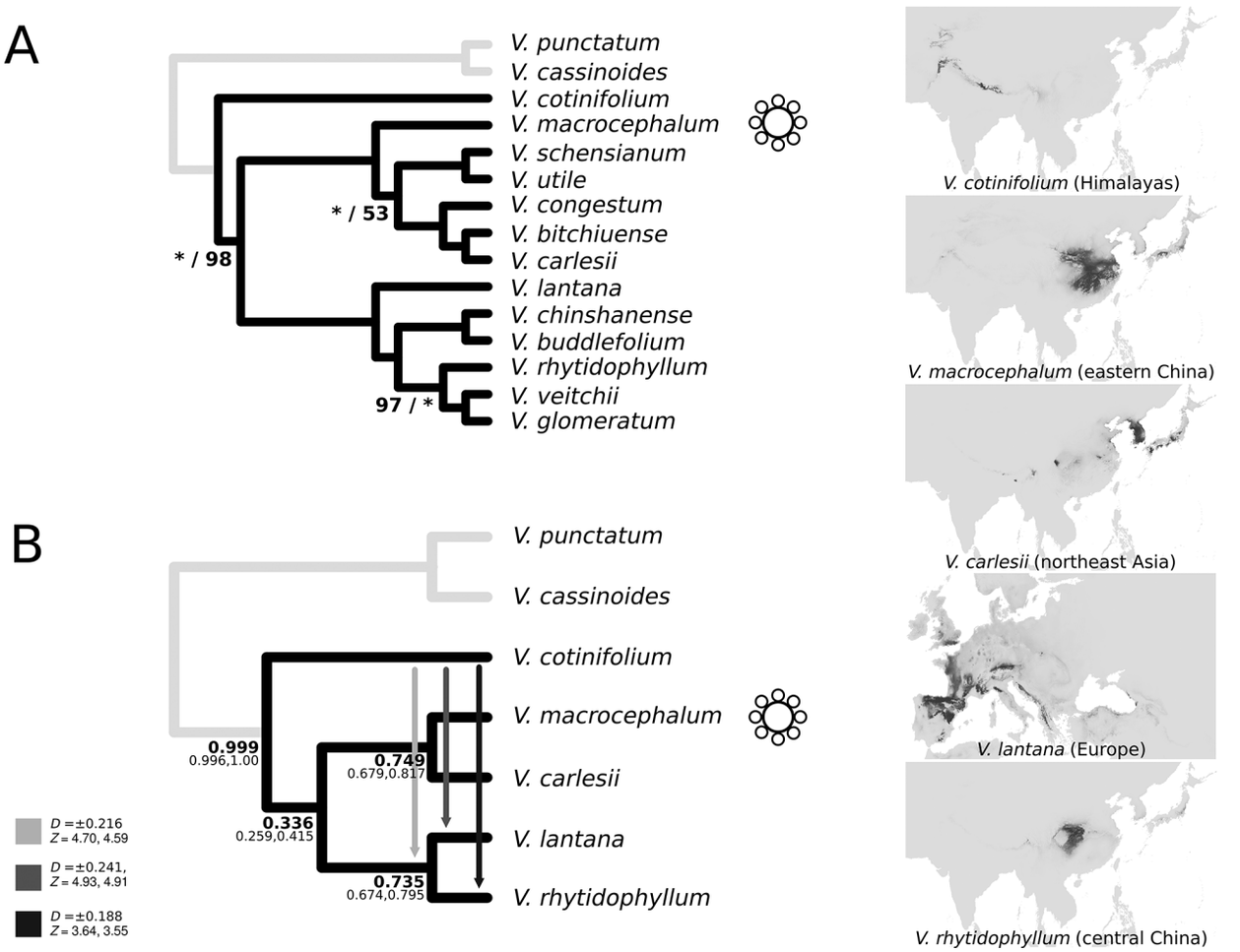

Fig. 7 *Euviburnum* phylogeny inferred from RAD-seq data. Illustrated inflorescences denote sterile marginal flower–producing species. *A*, Relationships inferred from maximum likelihood (ML) and species-tree analyses of the min4 data set. All nodes were resolved with 100% bootstrap support (BS) unless noted; asterisks denote 100% BS. *B*, Concordance factors estimated using BUCKy at $\alpha = 1.0$ and instances of gene flow inferred through ABBA-BABA tests are displayed on the ML and species-tree topologies. Mean concordance factors (in bold) and 95% confidence intervals are displayed below each node. Arrows denote gene flow from *Viburnum cotinifolium* into *V. lantana* (dark gray arrow), *V. rhytidophyllum* (black arrow), and the common ancestor of *V. lantana-rhytidophyllum* (light gray arrow). For each instance of gene flow, *D* statistics and *Z*-scores are reported next to the boxes corresponding to each colored arrow. Range maps estimated using Maxent for species used in the BUCKy and ABBA-BABA analyses are shown on the right.

and *V. veitchii* and *V. glomeratum* (Yunnan to Ningxia and Anhui). Relationships within this clade are well resolved, with the exception of the relationship between *V. rhytidophyllum* and *V. veitchii* plus *V. glomeratum*, which is supported with 97% and 57% BS (ML) in the min4 (fig. 7*A*) and min-ingroup10 (data not shown) data sets, respectively.

In contrast to the other SMF clades, the primary concordance tree inferred from 1037 loci conflicted with the ML and species-tree analyses. Specifically, *V. cotinifolium* was resolved as sister to the clade containing *V. lantana* and *V. rhytidophyllum*; that is, it is nested within *Euviburnum* (CF = 0.375, 95% CI = 0.296–0.456; data not shown). However, this split overlapped with the placement of *V. cotinifolium* as sister to the rest of *Euviburnum* (fig. 7; CF = 0.336, 95% CI = 0.259–0.415), the relationship obtained in ML and species-tree analyses, and so this is the concordance tree presented in figure 7*B*. Other than the contentious position of *V. cotinifolium*, the two subclades within *Euviburnum*, *V. lantana-rhytidophyllum* (CF = 0.735, 95% CI = 0.674–0.795) and *V. macrocephalum-carlesii* (CF = 0.749, 95% CI = 0.679–0.817), are well supported (fig. 7*B*). Several relationships not represented in the ML and species-tree analyses were supported with CF > 0.10, as follows: a sister species relationship between *V. lantana* and *V. cotinifolium* (CF = 0.152, 95% CI = 0.104–0.205), *V. macrocephalum* as sister to the rest of *Euviburnum* (CF = 0.121, 95% CI = 0.078–0.178), and a sister species relationship between *V. carlesii* and *V. rhytidophyllum* (CF = 0.110, 95% CI = 0.071–0.151).

Multiple ABBA-BABA tests conducted on the five-species data set with 3077 loci identified a significant history of gene flow from *V. cotinifolium* into *V. lantana*, *V. rhytidophyllum*, and the ancestor of *V. lantana-rhytidophyllum* (fig. 7*B*). When *V. cotinifolium* was treated as the P3 (donor) lineage, the most significant test

indicated gene flow into *V. lantana* (P1 or P2: $D = \pm 0.216$, $Z = 4.70, 4.59$; $P < 0.001$), followed by the ancestor of *V. lantana-rhytidophyllum* (P1 or P2: $D = \pm 0.241$, $Z = 4.93, 4.91$; $P < 0.001$) and then *V. rhytidophyllum* (P1 or P2: $D = \pm 0.241$, $Z = 4.93, 4.91$; $P < 0.001$). Introgression between these species was unidirectional, as there were no significant signatures of gene flow when *V. cotinifolium* was treated as either the P1 or P2 lineage. We note that these results imply that the distribution of *V. cotinifolium* once overlapped with that of the ancestor (or some members) of the *V. rhytidophyllum-lantana* clade (fig. 7), which currently shows a disjunction between central China (e.g., *V. rhytidophyllum*) and Europe (*V. lantana*).

Demographic reconstructions in BPP suggest that the major lineages within *Euviburnum* were established in rapid succession shortly after its emergence (table 1). We note the broad overlap in the estimated crown age of *Euviburnum* (20.4 mya, 95% CI = 16.0–25.6 mya), the divergence between *V. cotinifolium* and the rest of *Euviburnum* (20.1 mya, 95% CI = 15.8–25.3 mya), the origin of the *V. macrocephalum-carlesii* clade (19 mya, 95% CI = 14.1–24.9 mya), and the origin of the *V. lantana-rhytidophyllum* clade (16.4 mya, 95% CI = 6.20–23.8 mya). This is consistent with the short internodes along the backbone of the *Euviburnum* phylogeny estimated under ML. There was an estimated threefold reduction in effective population size between the ancestor of *Euviburnum* ($N_e = 47.2 \times 10^3$, 95% CI = 28×10^3–67.3×10^3) and the ancestor of the two major clades within *Euviburnum* ($N_e = 16 \times 10^3$, 95% CI = 1.58×10^3–34.2×10^3), indicating a reduction in population size and genetic diversity following the divergence between *V. cotinifolium* and other *Euviburnum* species. We caution that our ABBA-BABA tests and demographic analyses were conducted only on a reduced five-species data set. Nevertheless, taken together, our findings suggest that both introgression and ILS have served to obscure phylogenetic relationships in *Euviburnum*.

Discussion

Number of Origins of SMFs in Viburnum

Phylogenetic and character analyses indicate that SMFs arose relatively recently in *Viburnum* (i.e., since the early to mid-Miocene) and that there were four independent origins. Only in one of the SMF-containing clades is there a very slight possibility of multiple origins or of a reversal (ML and stochastic mapping with ER and ARD transition models sometimes place the origin of SMFs at the base of *Pseudotinus*, implying two origins or a single reversal in the non-SMF species *V. nervosum*). Although less parsimonious, this reconstruction cannot be entirely dismissed, and it will be useful to learn more about the genetic and developmental underpinnings of SMFs and to compare *V. nervosum* to its close relatives with SMFs (see Jin et al. 2010; Li et al. 2017; Lu et al. 2017). In the meantime, we consider a straightforward loss of SMFs to be unlikely in this case. To our knowledge, there are no observations (in the literature, in the field, or in herbaria) of a non-SMF-producing individual within any SMF-producing species, indicating that such a mutation must be exceedingly rare or that the secondary loss of SMFs is not beneficial (Park et al. 2018). On the other hand, we know that there must have been mutations in SMF species that gave rise to individuals producing only SMFs, judging by the snowball forms of *V. macrocephalum*, *V. plicatum*, and *V. opulus* (fig. S1). It is intriguing that the fertile flowers of *V. nervosum* have what appear to be the largest corollas and, correspondingly, the smallest stamens in *Viburnum* (except for those few species with tubular corollas). These somewhat intermediate flowers of *V. nervosum* suggest the possibility either that these were transitional to SMFs or that there was a transference of some aspects of SMF development to the fertile flowers in this case.

Comparison of the Environmental Settings in Which SMFs Evolved

Our analyses find that, overall, SMFs are not significantly associated with a specific set of climatic conditions. However, these analyses reveal subtle patterns in climatic niche evolution across these origins. In *Pseudotinus* and *Opulus*, our pPCA analyses indicated that both the SMF and non-SMF species are among the most cold-adapted species of *Viburnum*, occupying cool-temperate deciduous forests and cold conifer-dominated boreal forests in montane and northern Asia, eastern North America, and Europe. If SMFs had evolved only in these two lineages, it would be clear that their evolution was preceded by adaptation to cold climates, suggesting that these environments somehow favored the evolution of SMFs (e.g., to enhance pollination in areas with highly seasonal climates, where the availability and abundance of pollinators may vary from year to year; see Park et al. [2018] for the development of this argument for *V. lantanoides*).

Our findings for the other two SMF-containing lineages are broadly consistent with this idea, but the comparisons are not simple. The SMF-producing species *V. macrocephalum* and its non-SMF relatives within *Euviburnum* are certainly adapted to cool environments, occupying deciduous forests in eastern Asia (especially central China), westward in the Himalayas (*V. cotinifolium*), and in Europe (*V. lantana*). However, *V. macrocephalum* falls at the warmer end of the *Euviburnum* spectrum (fig. 3), and with a few exceptions (e.g., *V. mongolicum* and *V. burejaeticum*), species of *Euviburnum* do not occupy environments that are as cold as those inhabited by the species of *Pseudotinus* and *Opulus*, and there are other major *Viburnum* clades that occupy similar habitats and that never evolved SMFs.

The *Lutescentia* clade presents similar difficulties for a purely climatic hypothesis of SMF evolution. In this clade, the non-SMF species (e.g., *V. lutescens* and *V. pyramidatum*) occupy subtropical forests in Southeast Asia. *Viburnum plicatum* occupies more temperate forests at higher latitudes, and, to a lesser extent, so does *V. hanceanum*. These two SMF-producing species are adapted to cooler climates compared with most of their subtropical relatives (but see *V. amplifolium* in fig. 3), but they have not occupied especially cold environments in comparison with the species of *Pseudotinus* and *Opulus*. In this clade, the evolution of SMFs appears to have been phylogenetically coincident with the occupation of relatively colder climates, so it is unclear whether they evolved after the occupation of cold climates, as we surmise for *Pseudotinus* and *Opulus*.

In view of the incongruity in patterns of climatic niche evolution between *Pseudotinus* and *Opulus* on the one hand and *Euviburnum* and *Lutescentia* on the other, especially in the degree to which they have shifted into colder climates, it is not

surprising that we do not find an overall significant correlation with climate when we consider all four origins. As described above, we carried out several additional tests to better understand the effects of particular clades and species on the outcome of the climate correlation tests. We found that when we scored *V. hanceanum* and *V. plicatum* as lacking SMFs, the correlations between SMF-producing species and Bio06, as well as between SMF-producing species and "seasonal" climates, became significant. Significant results were also obtained when *V. macrocephalum* of *Euviburnum* was rescored as lacking SMFs. Taken together, these sensitivity analyses indicate that there is a significant correlation with cooler climates when only the six SMF species of *Pseudotinus* and *Opulus* are included. The three SMF species of *Lutescentia* and *Euviburnum* do not live in such cold climates, and it is their inclusion that yields an overall lack of significance.

Overall, it appears to us that at least relatively colder climates are correlated with the evolution of SMFs. *Pseudotinus* and *Opulus* shifted into very cold climates. In *Euviburnum* and *Lutescentia*, there were overall shifts in the direction of colder climates compared with related *Viburnum* species, but these shifts were far less extreme. In *Pseudotinus* and *Opulus*, a shift into cold climates was quickly followed by the evolution of SMFs, consistent with the view that SMFs are particularly advantageous in highly seasonal climates, where the availability of pollinator services can be highly variable (e.g., Schemske et al. 1978; Barrett and Helenurm 1987; Helenurm and Barrett 1987; Park et al. 2018). In *Euviburnum* this pattern is not so clear—cold climates were occupied before SMFs appeared, but the connection is not very direct (i.e., there was a long lag time). In *Lutescentia*, SMFs are inferred to have evolved in tandem with a shift into cooler, more seasonal climates relative to those of their more subtropical ancestors, so it is not possible to establish a clear sequence of events.

Two other observations are relevant here. First, there are *Viburnum* species living in quite cold climates that have not evolved SMFs (e.g., some species in the *Lentago*, *Dentata*, *Lobata*, and *Succotinus* clades). SMFs are clearly not necessary in such habitats, but why have they not evolved in these other cases? One possibility is that SMFs are not so advantageous for members of clades that have not evolved specialized growth patterns that cluster the inflorescences. That is, it may be that a particular combination of climatic niche and growth pattern favors the evolution of SMFs and that SMFs will not evolve in the absence of this combination. Another possibility is that SMFs have not evolved in these other cold-adapted species because an evidently very rare mutation simply never arose in these lineages. Second, we note that there are no *Viburnum* species with SMFs in tropical, subtropical, or cloud forest environments. This suggests that SMFs do not confer an advantage in these much less seasonal circumstances or that other attributes of these forests (e.g., shade at the time of pollination) or of the *Viburnum* species living in these forests (e.g., lower population densities, the lack of specialized branching patterns) are not conducive to the evolution of SMFs.

Plant Architectures Associated with SMF Evolution

Reproductive displays, especially plant size and patterns of branching that influence the clustering and collective apparency of flowers and inflorescences, are in part a function of organismal structure (Harder and Prusinkiewicz 2013; Liao and Harder 2014). As a variety of different growth patterns have evolved in *Viburnum*, it makes sense to explore how these correlate with the evolution of SMFs. The ancestral (and by far the most common) growth patterns of *Viburnum* are characterized by the production of only one type of shoot: orthotropic shoots that point upward and typically terminate in an inflorescence. In three evolutionarily derived growth forms—the *opulus*, *furcatum*, and *plicatum* growth patterns—two distinct types of shoots are produced (fig. 2). For the purposes of our analyses, these three were lumped into a single category on the grounds that all three have the effect of creating a distinctive display of inflorescences that might influence the attractiveness of the floral display at the level of the whole organism and hence the effectiveness of SMFs in increasing insect visitation and, in turn, male and female reproductive success.

We tested the hypothesis that SMFs are phylogenetically correlated with the derived growth patterns, and we found strong support for this proposition. Indeed, all species of *Pseudotinus* express the *furcatum* growth pattern, all species of *Opulus* are characterized by the *opulus* growth pattern, and all species of *Lutescentia* possess the *plicatum* growth pattern. This distribution suggests the possibility that the evolution of any one of these derived growth forms served to predispose these lineages to the evolution of SMFs, perhaps because the attractive function and reproductive benefits of SMFs are amplified when inflorescences are clustered and positioned in specialized patterns on the plant (see Liao and Harder 2014). The one exception is *V. macrocephalum*, which, on the basis of our knowledge of this plant in botanical gardens, expresses the growth pattern characteristic of the entire *Euviburnum* clade, which does not entail differentiation into two different shoot types. However, *V. macrocephalum* is noteworthy within *Euviburnum* in another way that could have a similar bearing on the evolution of SMFs. It stands out in this clade in producing the largest/tallest plants—these are often small trees—compared with other species in *Euviburnum*, which characteristically produce smaller shrubs. Consequently, *V. macrocephalum* individuals can produce many more inflorescences per plant, and it is possible that the function of SMFs is amplified in this context as well.

Understanding Phylogenetic Patterns in Light of Biogeography

Crown age estimates for the SMF lineages agree reasonably well with those from prior studies of *Viburnum* (Spriggs et al. 2015; Landis et al. 2021), though in two cases our estimates are ~10–20 myr younger (*Opulus*) or older (*Lutescentia*) than previously reported ages (table 1). Nevertheless, all appear to have originated during the early to mid-Miocene (table 1), and we found no evidence of an earlier evolution of SMFs (i.e., in the Eocene of the Oligocene). It is also noteworthy that none of the SMF lineages contain more than three extant species with SMFs, and it appears unlikely that SMFs were a key innovation in the sense that they promoted an increased rate of diversification (Donoghue and Sanderson 2015; Spriggs et al. 2015).

The evolutionary histories of *Pseudotinus* and *Opulus* are strikingly similar (figs. 4, 5; table 1). In both clades, the SMF species form a clade estimated to have arisen ~9 mya, shortly after

the initial diversification of their respective crown clades (~10 mya; table 1). We found no evidence of introgression between any species within *Pseudotinus* or *Opulus*, which is unsurprising considering that most of these species occur in complete allopatry. When there is range overlap, the species occupy somewhat different habitats, which might prevent gene flow from occurring (e.g., between the North American species *V. edule* and *V. trilobum* of the *Opulus* clade). The *Pseudotinus* and *Opulus* clades also show dynamic demographic histories, with large (~3.5-fold) reductions in ancestral population sizes coinciding with the origin of SMFs (table 1).

The remarkable correspondences between *Pseudotinus* and *Opulus* may be related to their biogeographic histories. It is likely that their common ancestors were distributed in high-latitude cold-temperate and boreal forests that spanned the Northern Hemisphere during the mid-Miocene to late Miocene (Donoghue et al. 2001; Donoghue and Smith 2004; Landis et al. 2021). Like many species at high latitudes (Rapoport 1982), the ancestors of the *Pseudotinus* and *Opulus* clades likely had broad distributions and possibly had large population sizes (table 1). The rare mutations underlying SMFs may have arisen more frequently under these circumstances and, once expressed, would likely have increased in frequency under positive selection (Park et al. 2018). However, considering that cold-adapted higher-latitude species may have been more vulnerable to range size contractions due to climate change (Hewitt 2000) and given the notable reduction in population sizes that we infer in the ancestors of the SMF species (table 1), SMFs may have become fixed when populations contracted. Following such fixation, the ancestors of the SMF species may have expanded rapidly around the Northern Hemisphere.

The patterns in *Lutescentia* and *Euviburnum* differ from those in *Pseudotinus* and *Opulus*, but in some ways these patterns are similar to one another. In *Lutescentia*, the SMF species (*V. hanceanum* and *V. plicatum*) form a clade (fig. 6) that is estimated to have originated ~17 mya (table 1), well before the origins in the other clades but well after the establishment of crown *Lutescentia* (~23 mya; table 1). Population sizes appear to have been stable throughout the history of *Lutescentia* (table 1), but we have uncovered a signature of past introgression, with gene flow from the ancestor of *V. lutescens-amplifolium* into *V. hanceanum* (fig. 6). This is perhaps unsurprising, as the ancestor of *V. lutescens-amplifolium* may have overlapped with *V. hanceanum* in southern China and because, while all other SMF-producing species are diploids (2n = 18), *V. hanceanum* is an octoploid with 72 chromosomes (Egolf 1956, 1962; Moeglein et al. 2020).

Crown *Euviburnum* is estimated to have existed in the early Miocene (~20 mya; table 1), and the major lineages were probably established shortly thereafter. The Himalayan species *V. cotinifolium* was resolved as sister to a clade containing the remainder of *Euviburnum* (fig. 7). This core *Euviburnum* clade is divided into two subclades. In one of these clades, the SMF-producing *V. macrocephalum* appears as sister to *V. carlesii* and four other species that occupy cold deciduous forests from central China to Korea and Japan. The other clade contains the European *V. lantana* and five other species centered in the mountains of central and southwestern China. We found significant conflict with respect to the placement of *V. cotinifolium* that may be explained either by ILS (supported by the rapid divergences and large population sizes inferred at the base of *Euviburnum*; table 1) or by introgression from *V. cotinifolium* into the ancestor of *V. lantana-rhytidophyllum* (fig. 7*B*). Introgression might appear to be unlikely based on the currently isolated Himalayan distribution of *V. cotinifolium*, but we hypothesize that its range once overlapped with that of species in the *V. lantana-rhytidophyllum* clade, which is today spread from Europe through central China to Siberia.

Conclusions

Figure 8 summarizes our findings. We have substantiated four independent gains of SMFs in *Viburnum*, with only a very slim chance that SMFs were ever lost or significantly modified in one of the four clades (*Pseudotinus*). Two of the four SMF-containing clades—*Pseudotinus* and *Opulus*—show basically identical patterns with respect to the variables that we analyzed. Both clades shifted into colder forests and evolved a novel growth pattern. These shifts do not strictly coincide with the evolution of SMFs in the phylogeny. Instead, SMFs evolved later in both cases, suggesting that the earlier shifts in climate and plant architecture predisposed these two lineages to the evolution of SMFs. That is, they were "precursors" in the sense of Donoghue and Sanderson (2015). Of course, this also required the appearance of mutations for the production of SMFs, which may have been favored in what we infer to have been exceptionally large populations. The fixation of SMFs was perhaps related to population bottlenecks and subsequent range expansion around the Northern Hemisphere. These findings make sense in relation to our experiments on pollination in *V. lantanoides*, in which SMFs appear to confer a distinct advantage in highly seasonal climates, in which pollinator services may be unreliable (Park et al. 2018).

The other two SMF-containing lineages show different but variously overlapping climatic, plant architectural, and demographic patterns. In both *Lutescentia* and *Euviburnum*, there may have been shifts into cooler, more seasonal climates, but these are relative changes and certainly do not match those of *Pseudotinus* and *Opulus* in absolute magnitude. These climatic shifts also did not clearly or closely precede the evolution of SMFs. In *Lutescentia*, a shift to a novel branching pattern did precede the evolution of SMFs (as in *Pseudotinus* and *Opulus*), but it seems that no such change occurred in advance of the evolution of SMFs within *Euviburnum* (although an increase in plant size in *V. macrocephalum* may have been a factor). *Lutescentia* and *Euviburnum* also differ from *Pseudotinus* and *Opulus* in being older crown clades that contain some species with overlapping geographic distributions and, consequently, in showing clear signs of past hybridization (figs. 6, 7*B*).

It appears from these analyses that no single factor has promoted the evolution of SMFs in all four cases of their evolution in *Viburnum*. Instead, a confluence of several factors may have triggered SMF evolution (Donoghue and Sanderson 2015). Yet it is clear that these factors occur in different combinations and likely evolved in different sequences in different clades. It is striking that *Pseudotinus* and *Opulus* show almost identical patterns, and a common causal explanation seems appropriate and satisfying in these two cases. *Lutescentia* is at least consistent with this pattern, and it is especially noteworthy that the double-file arrangement of inflorescences may have promoted the evolution of SMFs in this case. The addition of SMFs to

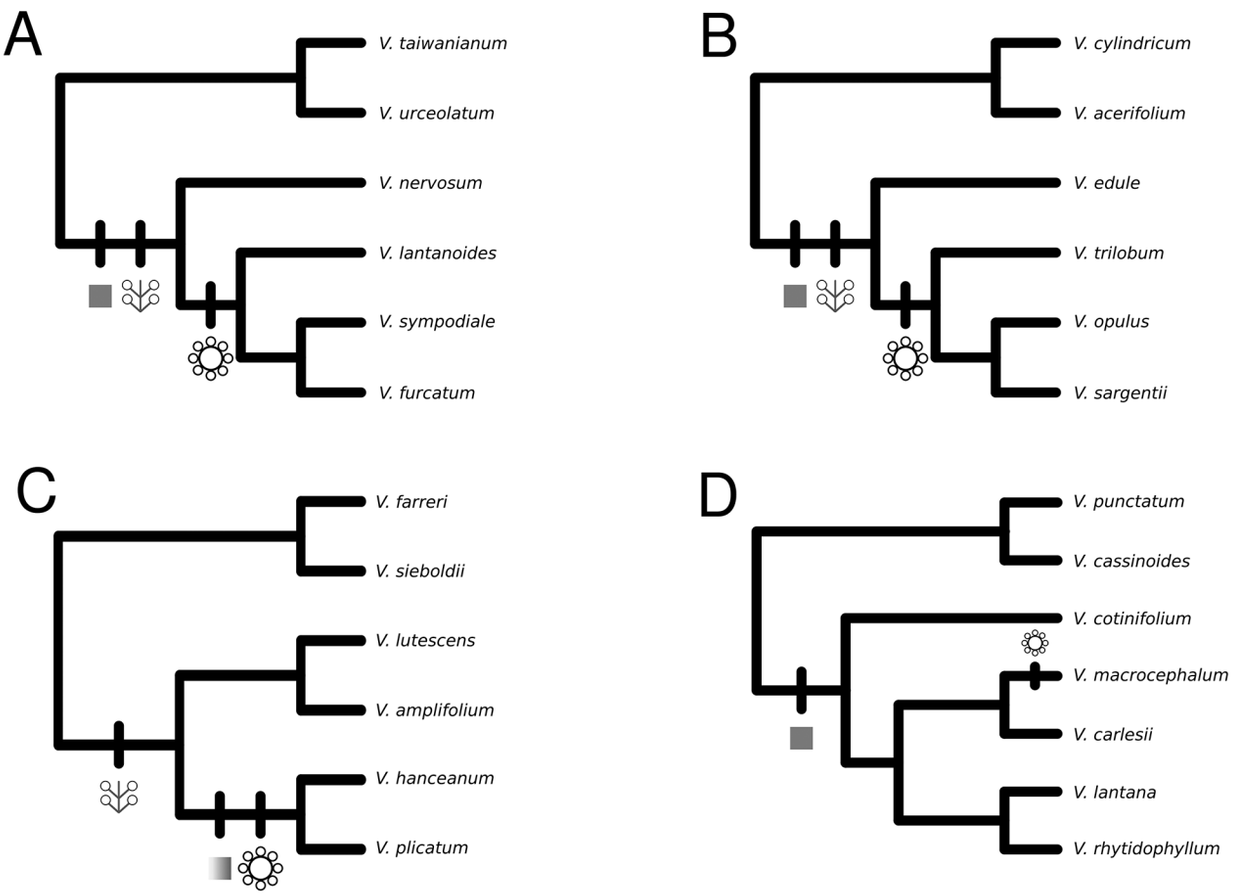

Fig. 8 Inferred sequences of character changes in the sterile marginal flower (SMF) lineages. *A*, In *Pseudotinus*, transitions into cool seasonal climates (square) and the evolution of sympodial plagiotropic branching (illustrated inflorescence) preceded the evolution of SMFs in the ancestor of *Viburnum lantanoides-sympodiale-furcatum*. *B*, Similar sequence as observed in *Opulus*, with transitions into cold highly seasonal climates and the evolution of specialized reproductive shoots. *C*, "Double-file" growth pattern is inferred to have evolved in the ancestor of *Lutescentia*, but transitions into cooler climates from more subtropical and tropical ancestors (square) roughly coincided with the evolution of SMFs in the ancestor of *V. hanceanum-plicatum*. *D*, In *Euviburnum*, adaptation to cold climates was not directly associated with SMF evolution, although it did precede it, and a specialized growth pattern did not evolve in this clade.

inflorescences in this arrangement may have greatly increased the attractiveness of the display at the whole-plant level. The need for some combination of these factors (i.e., climatic, organismal, historical) to be present before SMFs are favored may also help explain why other cold-adapted lineages of *Viburnum* (e.g., *Lentago*, *Dentata*, etc.) have not evolved SMFs. Of course, we cannot rule out other untested factors such as, perhaps, the greater attractiveness of showy inflorescences to herbivorous insects. *Viburnum macrocephalum*, the sole SMF-producing species in the *Euviburnum* clade, remains the biggest mystery. It occupies temperate forests, but it does not stand out as having adapted to especially cold conditions. Plants of *V. macrocephalum* do stand out in being larger and producing more inflorescences than their relatives, but they do not seem novel in terms of their branching pattern. Field studies and a better knowledge of the relevant environmental factors are clearly needed to understand the circumstances that may have favored SMFs in this particular case. This being said, we believe that the evolution of SMFs in *Viburnum* presents a highly nuanced case of parallel evolution in which relatively distantly related species proceeded along similar evolutionary trajectories from slightly different environmental and morphological starting points to achieve the same evolutionary ends (Revell et al. 2007). We hope that our detailed analyses of all four cases of the parallel evolution of SMFs in *Viburnum* provide a clear demonstration of the complexity surrounding the evolution of even the simplest and most obviously adaptive traits. If nothing else, our results highlight that there is a risk in extending a single causal adaptive explanation to every instance of a trait that evolved in parallel.

Acknowledgments

We thank Michael Landis for his efforts in generating the *Viburnum* phylogeny used in our broad comparative analyses. We also thank Erika Edwards, Thomas Near, and Simon Queenborough for helping us to interpret our results and improving the manuscript. This work was funded in part by a National Science Foundation award to M. J. Donoghue (IOS-1256706).

Literature Cited

Ané C, B Larget, DA Baum, SD Smith, A Rokas 2007 Bayesian estimation of concordance among gene trees. Mol Biol Evol 24:412–426.

Avni E, R Cohen, S Snir 2015 Weighted quartets phylogenetics. Syst Biol 64:233–242.

Barrett SCH, K Helenurm 1987 The reproductive biology of boreal forest herbs. I. Breeding systems and pollination. Can J Bot 65:2036–2046.

Baum DA 2007 Concordance trees, concordance factors, and the exploration of reticulate genealogy. Taxon 56:417–426.

Beaulieu JM, BC O'Meara, MJ Donoghue 2013 Identifying hidden rate changes in the evolution of a binary morphological character: the evolution of plant habit in campanulid angiosperms. Syst Biol 62:725–737.

Bell MA, G Orti, JA Walker, JP Koenings 1993 Evolution of pelvic reduction in threespine stickleback fish: a test of competing hypotheses. Evolution 47:906.

Chifman J, L Kubatko 2014 Quartet inference from SNP data under the coalescent model. Bioinformatics 30:3317–3324.

Clement WL, M Arakaki, PW Sweeney, EJ Edwards, MJ Donoghue 2014 A chloroplast tree for *Viburnum* (Adoxaceae) and its implications for phylogenetic classification and character evolution. Am J Bot 101:1029–1049.

Clement WL, MJ Donoghue 2011 Dissolution of *Viburnum* section Megalotinus (Adoxaceae) of Southeast Asia and its implications for morphological evolution and biogeography. Int J Plant Sci 172:559–573.

Conte GL, ME Arnegard, CL Peichel, D Schluter 2012 The probability of genetic parallelism and convergence in natural populations. Proc R Soc B 279:5039–5047.

Cresko WA, A Amores, C Wilson, J Murphy, M Currey, P Phillips, MA Bell, CB Kimmel, JH Postlethwait 2004 Parallel genetic basis for repeated evolution of armor loss in Alaskan threespine stickleback populations. Proc Natl Acad Sci USA 101:6050–6055.

Donoghue MJ 1981 Growth patterns in woody plants with examples from the genus *Viburnum*. Arnoldia 41:2–23.

——— 1982 Systematic studies in the genus *Viburnum*. PhD diss. Harvard University, Cambridge, MA.

Donoghue MJ, BG Baldwin, J Li, RC Winkworth 2004 *Viburnum* phylogeny based on chloroplast trnK intron and nuclear ribosomal ITS DNA sequences. Syst Bot 29:188–198.

Donoghue MJ, CD Bell, J Li 2001 Phylogenetic patterns in Northern Hemisphere plant geography. Int J Plant Sci 162(suppl):S41–S52.

Donoghue MJ, CD Bell, RC Winkworth 2003 The evolution of reproductive characters in Dipsacales. Int J Plant Sci 164(suppl): S453–S464.

Donoghue MJ, MJ Sanderson 2015 Confluence, synnovation, and depauperons in plant diversification. New Phytol 207:260–274.

Donoghue MJ, SA Smith 2004 Patterns in the assembly of temperate forests around the Northern Hemisphere. Philos Trans R Soc B 359:1633–1644.

Durand EY, N Patterson, D Reich, M Slatkin 2011 Testing for ancient admixture between closely related populations. Mol Biol Evol 28:2239–2252.

Eaton DAR 2014 PyRAD: assembly of de novo RADseq loci for phylogenetic analyses. Bioinformatics 30:1844–1849.

Eaton DAR, RH Ree 2013 Inferring phylogeny and introgression using RADseq data: an example from flowering plants (*Pedicularis*: Orobanchaceae). Syst Biol 62:689–706.

Eaton DAR, EL Spriggs, B Park, MJ Donoghue 2017 Misconceptions on missing data in RAD-seq phylogenetics with a deep-scale example from flowering plants. Syst Biol 66:399–412.

Edwards EJ, DS Chatelet, B-C Chen, JY Ong, S Tagane, H Kanemitsu, K Tagawa, et al 2017 Convergence, consilience, and the evolution of temperate deciduous forests. Am Nat 190(suppl):S87–S104.

Edwards EJ, DS Chatelet, L Sack, MJ Donoghue 2014 Leaf life span and the leaf economic spectrum in the context of whole plant architecture. J Ecol 102:328–336.

Edwards EJ, CP Osborne, CAE Strömberg, SA Smith, C_4 Grasses Consortium, WJ Bond, P-A Christin, et al 2010 The origins of C_4 grasslands: integrating evolutionary and ecosystem science. Science 328:587–591.

Edwards EJ, SA Smith 2010 Phylogenetic analyses reveal the shady history of C_4 grasses. Proc Natl Acad Sci USA 107:2532–2537.

Egolf DR 1956 Cytological and interspecific hybridization studies in the genus *Viburnum*. PhD diss. Harvard University, Cambridge, MA.

——— 1962 A cytological study of the genus *Viburnum*. J Arnold Arbor 43:132–172.

Englund R 1994 Male and female reproductive success in the hermaphroditic shrub *Viburnum opulus* (Caprifoliaceae). PhD diss. Uppsala University, Sweden.

Fick SE, RJ Hijmans 2017 WorldClim 2: new 1-km spatial resolution climate surfaces for global land areas. Int J Climatol 37:4302–4315.

Garland T, AW Dickerman, CM Janis, JA Jones 1993 Phylogenetic analysis of covariance by computer simulation. Syst Biol 42:265–292.

Green RE, J Krause, AW Briggs, T Maricic, U Stenzel, M Kircher, N Patterson, et al 2010 A draft sequence of the Neandertal genome. Science 328:710–722.

Hara H 1983 A revision of Caprifoliaceae of Japan with reference to allied plants in other districts and the Adoxaceae. Academia Scientific, Tokyo.

Harder LD, P Prusinkiewicz 2013 The interplay between inflorescence development and function as the crucible of architectural diversity. Ann Bot 112:1477–1493.

Helenurm K, SCH Barrett 1987 The reproductive biology of boreal forest herbs. II. Phenology of flowering and fruiting. Can J Bot 65:2047–2056.

Hewitt G 2000 The genetic legacy of the Quaternary ice ages. Nature 405:907–913.

Hijmans RJ 2017 raster: geographic data analysis and modeling. R package version 2.6-7.

Hijmans RJ, SJ Phillips, JR Leathwick, J Elith 2017 dismo: species distribution modeling. R package version 1.1-4.

Huelsenbeck JP, R Nielsen, JP Bollback 2003 Stochastic mapping of morphological characters. Syst Biol 52:131–158.

Huelsenbeck JP, F Ronquist 2001 MRBAYES: Bayesian inference of phylogenetic trees. Bioinformatics 17:754–755.

Ingvarsson PK 2008 Multilocus patterns of nucleotide polymorphism and the demographic history of *Populus tremula*. Genetics 180:329–340.

Jin B, L Wang, J Wang, N-J Teng, X-D He, X-J Mu, Y-L Wang 2010 The structure and roles of sterile flowers in *Viburnum macrocephalum* f. *keteleeri* (Adoxaceae). Plant Biol 12:853–862.

Kollman J, PJ Grubb 2002 *Viburnum lantana* L. and *Viburnum opulus* L. (*V. lobatum* Lam., *Opulus vulgaris* Borkh.). J Ecol 90:1044–1070.

Krannitz PG, MA Maun 1991*a* An experimental study of floral display size and reproductive success in *Viburnum opulus*: importance of grouping. Can J Bot 69:394–399.

——— 1991*b* Insect visitors to guelder rose, *Viburnum opulus* var. *opulus* (Caprifoliaceae) in London, Ontario. Can Field-Nat 105:13–17.

Landis MJ, DAR Eaton, WL Clement, B Park, EL Spriggs, PW Sweeney, EJ Edwards, MJ Donoghue 2021 Joint phylogenetic estimation of geographic movements and biome shifts during the global diversification of *Viburnum*. Syst Biol 70:67–85.

Larget BR, SK Kotha, CN Dewey, C Ané 2010 BUCKy: gene tree/species tree reconciliation with Bayesian concordance analysis. Bioinformatics 26:2910–2911.

Li W, Z He, L Zhang, Z Lu, J Xu, J Cui, L Wang, B Jin 2017 miRNAs involved in the development and differentiation of fertile and sterile flowers in *Viburnum macrocephalum* f. *keteleeri*. BMC Genomics 18:783.

Liao W-J, LD Harder 2014 Consequences of multiple inflorescences and clonality for pollinator behavior and plant mating. Am Nat 184:580–592.

Losos JB 2011 Convergence, adaptation, and constraint. Evolution 65:1827–1840.

Losos JB, TR Jackman, A Larson, K Queiroz, L Rodriguez-Schettino 1998 Contingency and determinism in replicated adaptive radiations of island lizards. Science 279:2115–2118.

Lu Z, J Xu, W Li, L Zhang, J Cui, Q He, L Wang, B Jin 2017 Transcriptomic analysis reveals mechanisms of sterile and fertile flower differentiation and development in *Viburnum macrocephalum* f. *keteleeri*. Front Plant Sci 8:261.

Maddison WP, DR Maddison 2018 Mesquite: a modular system for evolutionary analysis. Version 3.5.

Marazzi B, C Ané, MF Simon, A Delgado-Salinas, M Luckow, MJ Sanderson 2012 Locating evolutionary precursors on a phylogenetic tree. Evolution 66:3918–3930.

Mobley KB, D Lussetti, F Johansson, G Englund, F Bokma 2011 Morphological and genetic divergence in Swedish postglacial stickleback (*Pungitius pungitius*) populations. BMC Evol Biol 11:287.

Moeglein M, D Chatelet, MJ Donoghue, EJ Edwards 2020 Evolutionary dynamic of genome size in a radiation of woody plants (*Viburnum*). Am J Bot 107:1527–1541.

Nielsen R 2002 Mapping mutations on phylogenies. Syst Biol 51:729–739.

Pagel M 1994 Detecting correlated evolution on phylogenies: a general method for the comparative analysis of discrete characters. Proc R Soc B 255:37–45.

Park B, MJ Donoghue 2019 Phylogeography of a widespread eastern North American shrub, *Viburnum lantanoides*. Am J Bot 106:389–401.

Park B, M Sinnott-Armstrong, C Schlutius, J-CP Zuluaga, EL Spriggs, RG Simpson, E Benavides, et al 2018 Sterile marginal flowers increase visitation and fruit set in the hobblebush (*Viburnum lantanoides*, Adoxaceae) at multiple spatial scales. Ann Bot 123:381–390.

Phillips SJ, M Dudík, RE Schapire 2018 Maxent software for modeling species niches and distributions. Version 3.4.1. http://biodiversityinformatics.amnh.org/open_source/maxent/.

Rambaut A, MA Scuhard, D Xie, AJ Drummond 2014 Tracer. Version 1.6. http://beast.community/tracer.

Rannala B, Z Yang 2003 Bayes estimation of species divergence times and ancestral population sizes using DNA sequences from multiple loci. Genetics 164:1645–1656.

Rapoport EH 1982 Geographical areography. Pages 149–209 *in* EH Rapoport, ed. Areography. Pergamon, Oxford.

R Core Team 2018 R: a language and environment for statistical computing. R Foundation for Statistical Computing, Vienna.

Revell LJ 2009 Size-correction and principal components for interspecific comparative studies. Evolution 63:3258–3268.

——— 2011 phytools: an R package for phylogenetic comparative biology (and other things). Methods Ecol Evol 3:217–223.

Revell LJ, MA Johnson, JA Schulte II, JJ Kolbe, JB Losos 2007 A phylogenetic test for adaptive convergence in rock-dwelling lizards. Evolution 61:2898–2912.

Sage RF 2001 Environmental and evolutionary preconditions for the origin and diversification of the C_4 photosynthetic syndrome. Plant Biol 3:202–213.

Schemske DW, MF Willson, MN Melampy, LJ Miller, L Verner, KM Schemske, LB Best 1978 Flowering ecology of some spring woodland herbs. Ecology 59:351–366.

Sinnott-Armstrong MA, C Lee, WL Clement, MJ Donoghue 2020 Fruit syndromes in *Viburnum*: correlated evolution of color, nutritional content, and morphology in bird-dispersed fleshy fruits. BMC Evol Biol 20:7.

Spriggs EL, P-A Christin, EJ Edwards 2014 C_4 photosynthesis promoted species diversification during the Miocene grassland expansion. PLoS ONE 9:e97722.

Spriggs EL, WL Clement, PW Sweeney, S Madriñán, EJ Edwards, MJ Donoghue 2015 Temperate radiations and dying embers of a tropical past: the diversification of *Viburnum*. New Phytol 207:340–354.

Spriggs EL, DAR Eaton, PW Sweeney, C Schlutius, EJ Edwards, MJ Donoghue 2019*a* Restriction-site-associated DNA sequencing reveals a cryptic *Viburnum* species on the North American coastal plain. Syst Biol 68:187–203.

Spriggs EL, C Schlutius, DA Eaton, B Park, PW Sweeney, EJ Edwards, MJ Donoghue 2019*b* Differences in flowering time maintain species boundaries in a continental radiation of *Viburnum*. Am J Bot 106:833–849.

Stamatakis A 2014 RAxML version 8: a tool for phylogenetic analysis and post-analysis of large phylogenies. Bioinformatics 30:1312–1313.

Stayton CT 2015 The definition, recognition, and interpretation of convergent evolution, and two new measures for quantifying and assessing the significance of convergence. Evolution 69:2140–2153.

Stern DL 2013 The genetic causes of convergent evolution. Nat Rev Genet 14:751–764.

Winkworth RC, MJ Donoghue 2004 *Viburnum* phylogeny: evidence from the duplicated nuclear gene GBSSI. Mol Phylogenet Evol 33:109–126.

——— 2005 *Viburnum* phylogeny based on combined molecular data: implications for taxonomy and biogeography. Am J Bot 92:653–666.

Wong Sato A 2018 Diverse adaptations to increase pollination success in zoophilous plants. PhD diss. Kyoto University.

Yang Q-E, H Deyuan, D Boufford, V Malécot 2011 Adoxaceae. Pages 570–614 *in* ZY Wu, PH Raven, DY Hong, eds. Flora of China. Vol 19. Science, Beijing/Missouri Botanical Gardens, St Louis.